Available online at www.sciencedirect.com

SCIENCE DIRECT

Developmental Biology 284 (2005) 84 – 101

DEVELOPMENTAL BIOLOGY

www.elsevier.com/locate/ydbio

Exocrine pancreas development in zebrafish

Nelson S. Yee[a], Kristin Lorent[a], Michael Pack[a,b,*]

[a]Department of Medicine, University of Pennsylvania School of Medicine, Philadelphia, PA 19104-6058, USA
[b]Department of Cell and Developmental Biology, University of Pennsylvania School of Medicine, Philadelphia, PA 19104-6058, USA

Received for publication 29 October 2004, revised 5 April 2005, accepted 28 April 2005
Available online 16 June 2005

Abstract

Although many of the genes that regulate development of the endocrine pancreas have been identified, comparatively little is known about how the exocrine pancreas forms. Previous studies have shown that exocrine pancreas development may be modeled in zebrafish. However, the timing and mechanism of acinar and ductal differentiation and morphogenesis have not been described. Here, we characterize zebrafish exocrine pancreas development in wild type and mutant larvae using histological, immunohistochemical and ultrastructural analyses. These data allow us to identify two stages of zebrafish exocrine development. During the first stage, the exocrine anlage forms from rostral endodermal cells. During the second stage, protodifferentiated progenitor cells undergo terminal differentiation followed by acinar gland and duct morphogenesis. Immunohistochemical analyses support a model in which the intrapancreatic ductal system develops from progenitors that join to form a contiguous network rather than by branching morphogenesis of the pancreatic epithelium, as described for mammals. Contemporaneous appearance of acinar glands and ducts in developing larvae and their disruption in pancreatic mutants suggest that common molecular pathways may regulate gland and duct morphogenesis and differentiation of their constituent cells. By contrast, analyses of *mind bomb* mutants and *jagged* morpholino-injected larvae suggest that Notch signaling principally regulates ductal differentiation of bipotential exocrine progenitors.

Keywords: Exocrine pancreas; Zebrafish; Development; Duct; Acinus; Jagged; Notch

Introduction

The vertebrate pancreas serves dual physiological roles as both an exocrine gland for digestion and nutrition and an endocrine gland for glucose homeostasis. The exocrine pancreas is a lobulated organ comprised of acinar cells arranged in glands and a network of ducts that transport digestive enzymes secreted by acinar cells into the small intestine. Human diseases affecting the exocrine pancreas can arise from alterations affecting either ductular or acinar cells (reviewed by Bardeesy and DePinho, 2002; Lewis et al., 2003; Steer, 1997; Yee et al., 2003). Studies to define mechanisms underlying acinar and duct cell specification and cytodifferentiation and the developmental relationship of the glandular and ductular systems may provide clues to disease pathogenesis.

The morphogenetic events during vertebrate pancreas development have been well characterized. In amniotes, the pancreas arises from the endoderm as dorsal and ventral buds, which subsequently fuse to form a single anlage (Pictet and Rutter, 1972; Pictet et al., 1972; Slack, 1995; Wessells and Cohen, 1967). Signals from lateral plate mesoderm are believed to direct specification of the prepancreatic endoderm prior to bud formation (Kumar et al., 2003). Initially, the pancreatic anlage consists of a folded epithelium that is contiguous with the gut tube and is surrounded by mesenchyme. As development proceeds, the epithelium expands via branching morphogenesis to form what is generally considered the primitive ductal system. The primitive ducts are believed to give rise to endocrine cells that segregate to form islets and acinar glands that form at the terminal ends of these ducts. Mesenchymal signals to

* Corresponding author. Fax: +1 215 898 9871.
E-mail address: mpack@mail.med.upenn.edu (M. Pack).

0012-1606/$ - see front matter © 2005 Elsevier Inc. All rights reserved.
doi:10.1016/j.ydbio.2005.04.035

the pancreatic epithelium play an important role in this process (Gittes et al., 1996; reviewed by Kumar and Melton, 2003; Li et al., 2004).

Recently, this classical model of pancreas development, in which endocrine and acinar cells arise from pancreatic ducts, has been called into question by lineage tracing studies (Gu et al., 2003). These experiments support a model in which the three pancreatic lineages segregate within the pancreatic epithelium as it undergoes branching morphogenesis. Thus, the idea that endocrine and exocrine cells in embryos arise from progenitors already specified to form ducts may be misleading. Expression of the endocrine marker, *neurogenin-3* (Gu et al., 2002), within duct-like structures in the pancreatic epithelium underscores the difficulty of assigning pancreatic lineages based solely on histology (Pictet et al., 1972). A lack of early duct- and acinar-specific lineage markers further complicates these analyses.

Although the lineage relationships of endocrine, acinar and ductular progenitors within the pancreatic epithelium are not completely understood, some of the molecular signals that regulate endocrine and exocrine progenitors have been defined. The *pdx1* gene is expressed throughout the pancreatic epithelium and is required for the proliferation and differentiation of multipotent progenitor cells (Holland et al., 2002; Jonsson et al., 1994; Offield et al., 1996). Notch signaling appears to be required for progenitor cell maintenance. Notch inhibition, through targeting of the *delta-like 1 ligand*, *RBP-Jκ* (Apelqvist et al., 1999) or *hes-1* genes (Jensen et al., 2000), causes pancreatic progenitors to undergo precocious endocrine differentiation; as a result, Notch-deficient animals have pancreas hypoplasia. By contrast, activation of Notch signaling maintains progenitors in an undifferentiated state (Esni et al., 2004; Hald et al., 2003; Hart et al., 2003; Murtaugh et al., 2003; Norgaard et al., 2003). Finally, it has recently been shown that *FGF10*, a ligand normally secreted by pancreatic mesenchyme, regulates progenitor cell proliferation and maintenance, possibly through activation of the FGF receptor 2b (Bhushan et al., 2001; Miralles et al., 1999).

The identification of transcriptional regulators of endocrine lineage specification, such as the Notch target gene *neurogenin3*, led to the speculation that development of exocrine lineages is regulated in a related fashion. The gene encoding the p48 subunit of the PTF1 bHLH protein complex, *ptf1a*, was originally proposed to play such a role during exocrine differentiation because *ptf1a*$^{-/-}$ mutants lack acinar and ductular cells but retain endocrine cells (Krapp et al., 1998). However, recent studies show that *ptf1a* is expressed in multipotent pancreatic progenitors, and thus it is not an exclusive marker of cells committed to an exocrine fate (Kawaguchi et al., 2002). Consistent with this early role for *ptf1a*, *pdx1* deficiency, which arrests pancreatic progenitor development, can be rescued by expressing *pdx1* within cells that are normally *ptf1a*+ (Kawaguchi et al., 2002). These data suggest that *pdx1* and *ptf1a* may function coordinately during early stages of pancreas development to expand progenitor pools, possibly through interactions with the Notch signaling pathway (Obata et al., 2001).

Other than *ptf1a*, few genes have been identified as regulators of exocrine pancreas development (Cano et al., 2004; Pin et al., 2001). Such genes would be predicted to not only direct acinar and ductular lineage specification, but also later events such as cytodifferentiation and glandular and ductal morphogenesis. The zebrafish offers an attractive model system to identify such genes. Exocrine pancreas anatomy and physiology are conserved between teleost fish and mammals (Youson and Al-Mahrouki, 1999). Exocrine development in zebrafish and mammals each requires the *pdx1* and *ptf1a* genes (Lin et al., 2004; Yee et al., 2001; Zecchin et al., 2004). Furthermore, mutations affecting exocrine pancreas development independent of the endocrine pancreas have been recovered (Field et al., 2003; Mayer and Fishman, 2003; Pack et al., 1996). In this study, we present new data describing later stages of exocrine pancreas development. Using immunohistochemistry and ultrastructural analyses, we report the timing of acinar and ductular differentiation and morphogenesis. These data support a model of exocrine development in which acinar and ductular cells develop in situ from progenitors that are spatially segregated within the zebrafish pancreatic anlage at an earlier developmental stage. We also characterize exocrine differentiation, proliferation and morphogenesis in mutants in which pancreas development is perturbed and following knockdown of genes that play a role in mammalian pancreas development. These studies show that acinar and duct development are largely regulated in a coordinate fashion. However, Jagged-mediated Notch signaling appears to play a predominant role in duct development.

Materials and methods

Fish stock

Methods for raising and maintaining zebrafish stocks are described in detail elsewhere (Westerfield, 2000; Yee and Pack, 2004). The zebrafish AB strain was used to study normal development of exocrine pancreas. Embryos were raised in 10 cm petri dishes (maximum 60 fertilized embryos per dish) containing E3 medium supplemented with 0.6 μM methylene blue (Fisher Scientific) to inhibit growth of contaminating fungi and other organisms in an incubator at 28.5°C. To facilitate visualization of embryonic and larval zebrafish digestive organs in whole-mount preparations, skin pigmentation was inhibited by raising embryos and larvae in E3 medium containing 0.2 mM 1-phenyl-2-thiourea (PTU) (Sigma). The *slimjim* (*slj*^{m74}) and *piebald* (*pie*^{m497}) mutants were previously described by Pack et al. (1996), the *flotte lotte* (*flo*^{ti262c}) mutant by Chen

et al. (1996), and the *mind bomb* (*mib*^{m132}) mutant by Schier et al. (1996) and Itoh et al. (2003).

For Notch activation experiments, hemizygous *hsp70:-GAL4* and *UAS:notch1a-ICD* fish were mated as described (Esni et al., 2004; Scheer et al., 2001). Progeny were heat shocked at 40°C for 30 min every 12 h beginning at 72 hpf. Larvae were fixed at 120 hpf (5 dpf) and processed for immunohistochemistry as described below. Following phenotypic classification, Notch-activated larvae were genotyped by PCR for the *UAS:notch1a-ICD* transgene as described by Esni et al. (2004). Wild-type and transgenic siblings were processed for immunohistochemical analyses in parallel.

For ethanol treatment, wild type embryos were dechorionated using forceps at 10 hpf, incubated in 1.9% ethanol in E3 medium at 28.5°C up to 48 hpf, rinsed with E3 medium 3 times and then incubated in E3 medium for another 48 h, during which ethanol was removed to prevent severe developmental delay. Control embryos were incubated in E3 medium for a total of 96 h. The 4 dpf larvae were fixed and analyzed as described below.

Mutagenesis screen

Mutagenized fish were generated as described (Dosch et al., 2004; Wagner et al., 2004). F3 progeny corresponding to 350 F2 families were screened on 5 dpf by whole mount immunohistochemistry using anti-carboxypeptidase A and anti-insulin antibodies (see below). Mutant families showing altered carboxypeptidase A or insulin staining patterns that were transmitted in a recessive Mendelian pattern were selected for further analysis. Larvae that showed delayed growth or necrosis were discarded. Complementation analyses were conducted with all mutants. Four mutants with altered carboxypeptidase A staining patterns were identified: *sweetbread* (*swd*^{p75fm} and *swd*^{p82mf}), *mitomess* (*mms*^{p13cv}), *ductjam* (*djm*^{p26nb}) and *ducttrip* (*dtp*^{p14nb}).

Immunohistochemistry

Methods for whole-mount immunohistochemistry of zebrafish embryos and larvae were described in detail elsewhere (Yee and Pack, 2004). For carboxypeptidase A, amylase, insulin and cadherin immunohistochemistry, embryos and larvae were fixed with 4% paraformaldehyde (Fisher Scientific). Prior to incubation with primary antibodies, the rehydrated embryos were permeabilized with 0.1% collagenase (Sigma). For cytokeratin immunohistochemistry, larvae were fixed in methanol:dimethyl sulfoxide (4:1). Primary antibodies include rabbit anti-human amylase antibodies (Sigma), rabbit anti-bovine carboxypeptidase A antibodies (Rockland), guinea pig anti-insulin antibodies (Linco), mouse anti-human cytokeratin 18 monoclonal antibodies (Maine Biotechnology) and rabbit anti-pan cadherin antibodies (Sigma). The primary antibodies were diluted 1:100 with 5% goat serum (GibcoBRL) and incubated at 4°C overnight. Embryos were then washed with phosphate-buffered saline (PBS) containing 0.1% Tween-20, pH 7.0. Fluorescence-conjugated secondary antibodies (Molecular Probes) including Alexa® 488 or 568 nm goat anti-rabbit antibodies, Alexa® 488 or 568 nm goat anti-mouse antibodies and Alexa® 594 nm goat anti-guinea pig antibodies were used as secondary antibodies. The secondary antibodies were diluted 1:100 with 5% goat serum and incubated at 4°C overnight. Following incubation, the samples were washed 3 times in PBS containing Tween-20. The specimens were mounted in Vectashield® mounting medium for fluorescence (Vector Laboratories) and examined under fluorescent stereomicroscope (Leica MZFLIII). Confocal analyses of pancreatic ducts were performed using a laser scanning microscope (Zeiss).

In situ hybridization

Standard protocols are followed for in situ hybridization with antisense RNA probes and described in detail elsewhere (Yee and Pack, 2004). Briefly, a digoxigenin-labeled antisense riboprobe against *pdx1* (Wallace and Pack, 2003), *gata6* (Genbank AF191578; a gift of L. Zon; erroneously referred to as *gata-5* in Pack et al., 1996), *ptf1a* (Lin et al., 2004) and *trypsin* (Lin et al., 2004) was generated using SP6 or T7 RNA polymerase (Enzo). For in situ hybridization, the paraformaldehyde-fixed larvae were permeabilized using proteinase K (Roche) and hybridized with preadsorbed riboprobe at 68°C overnight. Following hybridization, the larvae were washed extensively using 3 M NaCl/0.3 M sodium citrate solution, pH 7.0 (SSC) (Mediatech, Inc.) at 68°C. The hybridized RNA was detected using anti-digoxigenin/alkaline phosphatase Fab fragments (Roche) followed by incubation with the substrates 4-Nitro blue tetrazolium chloride (NBT) (Enzo) and 5-Bromo-4-chloro-3-indolyl-phosphate (BCIP) (Enzo). The larvae were cleared in graded glycerol solutions to improve signal detection. Visual inspection of the specimen was performed using a stereo dissecting microscope (Leica MZ12) with overhead illumination from a halogen light source.

Hybridizations of mutant larvae and wild type siblings with *ptf1a* and *trypsin* antisense probes were performed at 48 hpf, 60 hpf, 72 hpf, 4 dpf and 5 dpf. *Ptf1a* and *trypsin* staining patterns of 48 hpf and 60 hpf in all mutants and wild type larvae were indistinguishable from one another.

Histological analysis

The preparation of histological sections was described in detail elsewhere (Yee and Pack, 2004). Briefly, the specimens were serially dehydrated with ethanol solutions and then embedded with JB-4 solution according to manufacturer's instruction (Polysciences). Sections of 3 μm thickness were prepared using a microtome (Leica Model RM2155). For light microscopic analysis, histological sections were

stained in methylene blue (Fisher Scientific)–azure II (Sigma) solution, rinsed with distilled water, mounted with Permount® (Fisher Scientific) and examined and photographed under a compound microscope (Axioskop) (Zeiss) using ProgRes 4.0 software. For fluorescent microscopic analysis, histological sections were mounted with Vectashield® mounting medium for fluorescence (Vector) and counterstained DNA with 4′,6 diamidino-2-phenylindole (dapi). Analyses and photography of the histological sections were performed under a compound microscope (Nikon Eclipse E600) using *IPLab New MP* software.

Electron microscopy

Larvae were fixed with 2.5% glutaraldehyde +2% paraformaldehyde in 0.1 M sodium cacodylate buffer pH 7.4, post fixed in 2% osmium tetraoxide, dehydrated in graded alcohol and embedded in EPON 812. Transverse sections of 70 nm thickness each were prepared using Ultracut S microtome (Leica) and examined under transmission electron microscope JEM 1010 (JEOL). Digital images were captured using Hamamatsu ORCA CCD camera aided by AMT 12-HR software. All materials were purchased from Electron Microscopy Sciences, and these procedures were conducted at the Biomedical Imaging Core Facility of the University of Pennsylvania.

Morpholino injection

Morpholinos (Gene Tools, LLC) were stored as a stock solution of 2 mM at −80°C and diluted with Danieau's buffer prior to injection (Yee and Pack, 2004). A combination of morpholinos against zebrafish *jagged2* (5′-tcctgatacaattccacatgccgcc-3′) and *jagged3* (5′-ctgaactccgtcgcagaatcatgcc-3′) were microinjected, each at a 1:10 dilution of the stock solution, into embryos at the 1-cell stage (Lorent et al., 2004).

Results

This work represents our initial efforts to define mechanisms of exocrine pancreas development. The goals of this work are to characterize the anatomy and ultrastructural features of the zebrafish acinar and ductal systems and to identify genes that regulate their development. Differentiated acinar cells were identified with anti-amylase and anti-carboxypeptidase A (cpa) antibodies and duct cells by anti-cytokeratin (cyk) antibodies. These and other markers used for this study are listed in Table 1.

Adult zebrafish exocrine pancreas anatomy

The exocrine pancreas of adult zebrafish is a diffuse organ comprised of a branching network of ducts and associated acinar glands that reside between adjacent loops of intestine (Fig. 1A). The exocrine ductal system arises as branches of the main pancreatic duct that inserts into the proximal intestine. We define segments or branches of exocrine tissue and their associated ducts as lobules (Fig. 1B). Histological analyses show that the exocrine lobules are comprised of acinar glands and large ducts lined by cuboidal cells (Figs. 1D, E). Cyk immunohistochemistry identifies the large ducts and small intercalated ducts associated with acinar glands (Fig. 1C). Vascular endothelial cells lining blood vessels are also cyk+ but can be distinguished from small intercalated ducts by their larger cross-sectional area and the presence of luminal blood cells. Ultrastructural analyses revealed that the exocrine glands (acini) are comprised of polarized cells containing apical zymogen granules that store digestive enzymes and abundant rough endoplasmic reticulum and mitochondria (Fig. 1F). Centroacinar cells, which are considered the most distal component of the intrapancreatic ductular system, were easily identified in electron micrographs by their location within the acinar lumen and characteristic scant cytoplasm (Fig. 1F). Together, these data show that exocrine morphology and ultrastructure are highly conserved between zebrafish and mammals.

Table 1
Cell-specific markers for zebrafish embryos and larvae

Markers	Expressing cells
Cytokeratin (cyk)	Pancreatic ductular epithelia, vascular endothelial cells
Amylase (amy)	Acinar cells, exocrine pancreas
Carboxypeptidase A (cpa)	Acinar cells, exocrine pancreas
Trypsin	Acinar cells, exocrine pancreas
Pancreas duodenum homeobox 1(*pdx1*)	Pancreatic endocrine and exocrine progenitors, rostral gut endoderm
gata6	Exocrine pancreas, liver and intestinal endodermal derivatives
Cadherin (cad)	Acinar, centroacinar and ductular cells, exocrine pancreas

Exocrine pancreas morphogenesis and cytodifferentiation during larval development

Given these similarities of zebrafish and mammalian exocrine pancreas anatomy, we speculated that mechanisms of acinar and ductular development were conserved during vertebrate evolution. To define exocrine development in zebrafish, we first characterized the timing of acinar and ductular cytodifferentiation and morphogenesis in embryos and larvae by in situ hybridization and immunohistochemistry using various markers listed in Table 1.

Zebrafish endocrine and exocrine progenitors are spatially segregated at early developmental stages (Biemar et al., 2001; Field et al., 2003, Fig. 2). Previous studies have shown that the *ptf1a* and *mnr2a* genes identify exocrine progenitors surrounding the solitary pancreatic islet at 48 hpf (Lin et al., 2004; Wendik et al., 2004; Zecchin et al., 2004). We term this structure and the contiguous extrapancreatic duct, the

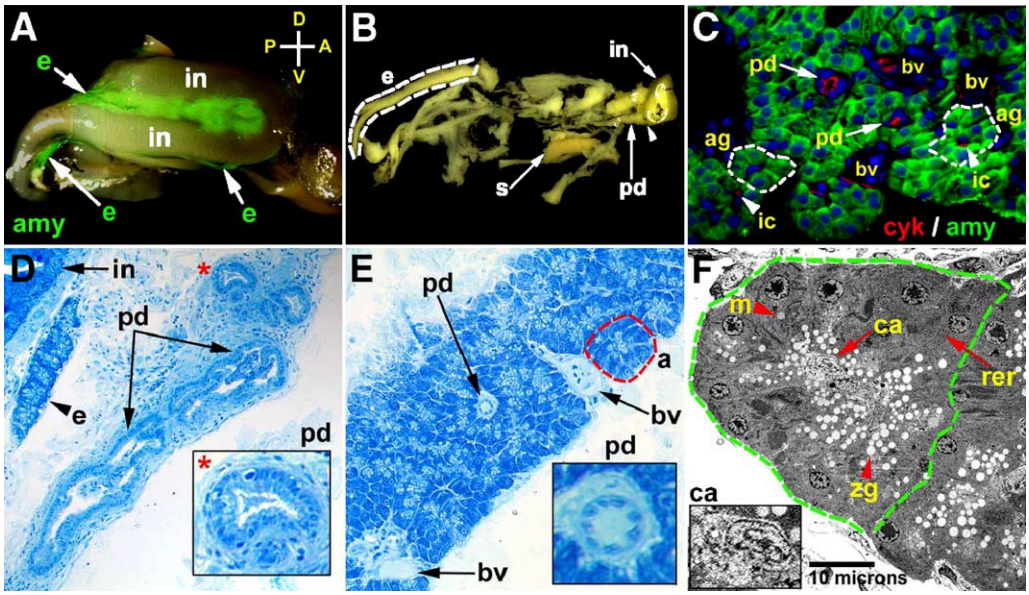

Fig. 1. Adult exocrine pancreas. (A) Whole mount image of the dissected adult zebrafish digestive tract, right lateral view, processed for amylase immunohistochemistry (IHC). Exocrine tissue (green) is identified between adjacent intestinal loops. (B) Adult zebrafish pancreas dissected from adherent intestinal tissue. This fixed specimen reveals the branched network of exocrine lobules and associated ducts. Arrowhead points to insertion site of the extrapancreatic duct to the intestine. An exocrine lobule is outlined by the dashed white line. (C) Histological section of adult pancreas processed for cytokeratin (red) and amylase (green) IHC; DNA counterstained with dapi (blue) to visualize cell nuclei. Dashed white lines outline two acinar glands. Arrows point to large pancreatic ducts within the lobule. Arrowheads point to intercalated ducts. (D) Sagittal histological section showing large pancreatic ducts with adjacent exocrine and intestinal tissues. (E) Histological section of an exocrine lobule showing acinar cells with a prominent duct. Insets (* in panel D; long arrow in panel E) show cuboidal cells lining these ducts. Red dashed line outlines an acinus. (F) Transmission electron micrograph showing an acinus comprised of polarized cells with apical zymogen granules, basal nucleus, mitochondria and rough endoplasmic reticulum. A centroacinar cell is identified based upon its position within the acinar lumen and its scant cytoplasm (inset). e: exocrine tissue; in: intestine; amy: amylase; s: spleen; ag: acinar glands; pd: pancreatic ducts; ic: intercalated ducts; bv: blood vessel; a: acinus; zg: zymogen granules; m: mitochondria; rer: rough endoplasmic reticulum; ca: centroacinar cell; A: anterior; P: posterior; D: dorsal; V: ventral.

exocrine anlage. At this stage, exocrine cells also express *gata6* (data not shown) and the acinar marker *trypsin* RNA (Lin et al., 2004; data not shown), but lack cpa protein (Figs. 3A and B), and thus appear to be analogous to the protodifferentiated progenitors within the mammalian pancreatic epithelium first described by Pictet et al. (1972). By contrast, cells of the extrapancreatic duct at this stage (48 hpf) are cyk+ (Figs. 3A and B). Between 50 hpf and 52 hpf, *gata6*+ exocrine tissue caudal to the *pdx1*+ islet expands to form what we term the tail of the larval pancreas (Figs. 2C and D). We find that acinar cytodifferentiation is initiated at this stage in some larvae, as indicated by weak cpa immunoreactivity (not shown) that is robust at 60 hpf (Figs. 3C and D). Small cyk+ cells embedded within clusters of cpa+ cells not yet arranged in acini (discussed below) are also first identified at this stage (Figs. 3C and D). Histological analysis shows that these small cyk+ cells are not contiguous with the extrapancreatic duct. Taken together, these data argue that acinar and ductular cytodifferentiation in the rostral pancreas, which we term the pancreatic head, precedes glandular and duct morphogenesis.

At 72 hpf, exocrine tissue surrounding the islet (Fig. 2E) has expanded, and the tail of exocrine tissue extending from the pancreatic head to the caudal region of the swim bladder is well formed (Fig. 2F). Cyk immunohistochemistry identifies discontinuous segments of the small intrapancreatic ducts within the pancreatic tail at this time point (Figs. 4A–D). These small primary ducts are oriented longitudinally, along the anterior–posterior axis of the pancreas. A related pattern of acinar cells and associated ducts is evident in the pancreatic head at this stage, although it is less obvious because the islet and its prominent vasculature, which is also cyk+, partially obscure the ductular network (data not shown). Ultrastructural analysis at this stage revealed acinar glands in the pancreatic tail were comprised of cuboidal cells with few zymogen granules (Fig. 5A).

Between 72 hpf and 96 hpf, there is continued expansion and differentiation of exocrine cells in both the pancreatic head and tail (Figs. 4E–H). At 96 hpf, first order branches of pancreatic ducts are identified (Figs. 4I–L). Electron micrographs reveal that acinar cells develop a pronounced columnar morphology with prominent zymogen granules during this period (Figs. 5A–C). Tight junctions between adjacent acinar cells are also evident (data not shown), and centroacinar cells are easily identified in the center of all glands (Fig. 5C). At 120 hpf (5 dpf), acinar cells appear fully polarized (Fig. 5D). Cyk immunohistochemistry at this stage reveals an organized network of ducts including second order branches that drain individual acini (Figs. 4M–P). Interestingly, a main intrapancreatic duct was evident in fewer than 50% of larval pancreata analyzed, and when it was apparent in these larvae, the duct was

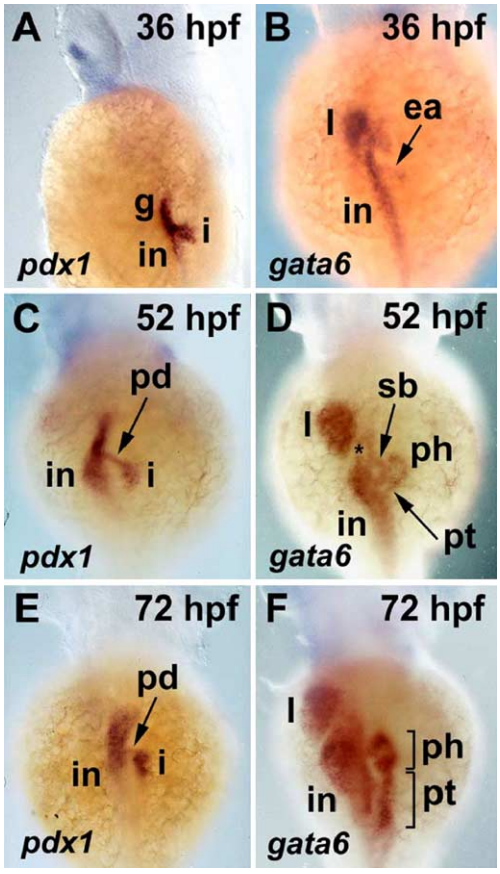

Fig. 2. *pdx1* and *gata6* expression in the developing zebrafish pancreas and digestive tract; whole mount RNA in situ hybridization, dorsal view. (A, B) At 36 hpf, *pdx1* expression in the pancreatic islet, intestine and rostral gut endoderm is evident; *gata6* is expressed in the intestine, liver and in the exocrine anlage. (C, D) At 52 hpf, *pdx1* is expressed in cells of the endocrine pancreas and a stalk of tissue corresponding to the extrapancreatic duct. Histological sections (not shown) show exocrine cells adjacent to the islet also express *pdx1*. *gata6* is expressed in exocrine cells surrounding the islet that forms the pancreatic head. Tissue of the pancreatic tail is first visible at this stage. (*) pancreatic duct insertion site. (E, F) By 72 hpf, the exocrine pancreas has grown significantly; *pdx1* expression in the pancreatic duct is diminished. i: pancreatic islet; in: intestine; g: gut endoderm; l: liver; ea: exocrine anlage; pd: pancreatic duct; sb: swim bladder; ph: pancreatic head; pt: pancreatic tail.

discontinuous (Figs. 4O and P). In larvae without such segmented main ducts, individual acini were linked to one another and the extrapancreatic duct by a network of small interconnecting ducts (examples in Figs. 9A5 and A6).

Although cpa immunohistochemistry allowed us to visualize acinar cells, acinar gland morphogenesis was difficult to appreciate in routine histological sections or tissue sections of cpa-stained embryos and larvae. To better understand, the timing of gland morphogenesis, we used cadherin immunohistochemistry to define acinar structure. The cadherin immunostainings outlined the basolateral border of acinar cells and the small centrally located centroacinar cells. Tissue sections of 48 hpf and 60 hpf cadherin stained larvae identified immature acini rostral to the islet (Figs. 6A and B). Well-defined acini were first observed at 72 hpf in this location (Fig. 6C). By contrast, posterior (tail) exocrine cells at this stage appeared to be arranged in contiguous longitudinally aligned acini (Fig. 6E). At 84 hpf, lobulation of the exocrine tissue rostral to the islet was evident (Fig. 6D), and multiple acini were now evident in the pancreatic tail (Fig. 6F). Between 84 hpf and 120 hpf, there is marked expansion of the exocrine tissue; cadherin immunostainings at this stage reveal numerous small acini in the pancreatic head (data not shown) and tail (Figs. 6G and H).

The morphological changes and ultrastructural features of the exocrine pancreas during embryonic and larval development are summarized in Table 2.

Morphogenetic mechanisms underlying exocrine pancreas development

The mammalian pancreas develops from dorsal and ventral anlagen that arise from foregut endoderm. These tissue buds are comprised of epithelial evaginations, perpendicular, but contiguous with the adjacent prospective intestinal endoderm. Although the lineage relationships within the pancreatic epithelium have not been completely characterized, it is generally believed that acini develop at the terminal branches of the pancreatic duct-like epithelium, whereas the endocrine cells segregate from the epithelium to form islets at early stages (Gu et al., 2003; Pictet and Rutter, 1972). Zebrafish exocrine and endocrine pancreas develop from distinct, spatially segregated rostral and caudal anlagen (Fig. 2; Biemar et al., 2001; Field et al., 2003; Lin et al., 2004; Zecchin et al., 2004). Cadherin immunohistochemistry suggests a different organization of cells within the exocrine anlage. At 48 hpf, the extrapancreatic duct is arranged as a simple epithelium (Figs. 3A and B). Based upon morphology, we consider this structure to be analogous to the mammalian pancreatic epithelium. However, in zebrafish, exocrine tissue contiguous with the duct appears to be arranged as a stratified rather than a simple epithelium (Fig. 6A; Supplementary Fig. 1). Over time, this arrangement of cells resolves into a well-defined acinar pattern with associated small ducts (Figs. 3C and D, 6A–H). Thus, zebrafish pancreatic acini appear to form in situ, from exocrine progenitors that are not arranged as a simple epithelium.

Staged cyk immunostainings suggest a similar mechanism for duct formation (Figs. 3 and 4). These data show that ducts within the zebrafish pancreas originally arise in situ from isolated progenitor cells rather than arising from reiterative branching of the pancreatic epithelium. This process of pancreatic duct formation in zebrafish may be analogous to the mechanism of duct formation in the mammalian mammary and salivary glands (Hieda et al., 1996; Hogg et al., 1983). Here, non-polarized cells within a stratified branching epithelium rearrange to form small lumens that subsequently join to form a tubular network of primitive ducts. A related mechanism of duct formation has also been

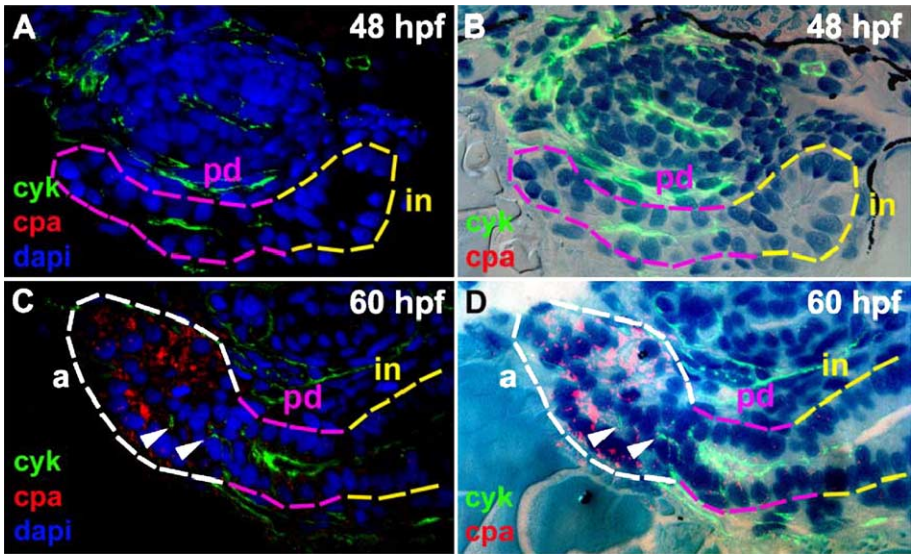

Fig. 3. Exocrine differentiation and gland morphogenesis. (A–D) Histological cross-sections of 48 hpf (A) and 60 hpf (C) larvae processed for whole mount cpa and cyk immunohistochemistry (IHC) and dapi. (B and D) Merged fluorescent images without dapi staining (A and C) and bright field images of the corresponding histological sections stained with methylene blue and azure II. The main pancreatic duct (pink outline) is contiguous with the intestine (in, yellow outline) at 48 hpf. Cpa expression is evident in exocrine cells forming a primitive acinus-like structure at 60 hpf (white outline). Cyk+ duct cells (arrowheads) are present adjacent to the developing acinus but are not contiguous with the extrapancreatic duct in this and adjacent sections (not shown). cpa: carboxypeptidase A; cyk: cytokeratin; pd: pancreatic duct; a: acinus; in: intestine.

proposed to occur within the mammalian pancreatic epithelium (Hogan and Kolodziej, 2002; Jensen, 2004).

Given these potential differences between the developing zebrafish and mammalian intrapancreatic ductal systems, we next examined the relationship of ductal progenitors to the gut epithelium. Although we found no histological evidence of expansion and branching of zebrafish exocrine progenitors into surrounding mesenchyme, previous work (Field et al., 2003) suggests that the exocrine anlage arises as a bud of cells from either a rod of rostral endoderm or the rostral gut tube (intestinal anlage) itself, between 32 hpf and 34 hpf. An alternative model of exocrine development posits that the exocrine anlage arises independently of the gut epithelium and joins the rostral intestine at subsequent stages (Wallace and Pack, 2003). Fusion of the exocrine anlage with the intestine, and subsequent anlage growth, could resemble tissue budding described in staged, real-time observations (Field et al., 2003).

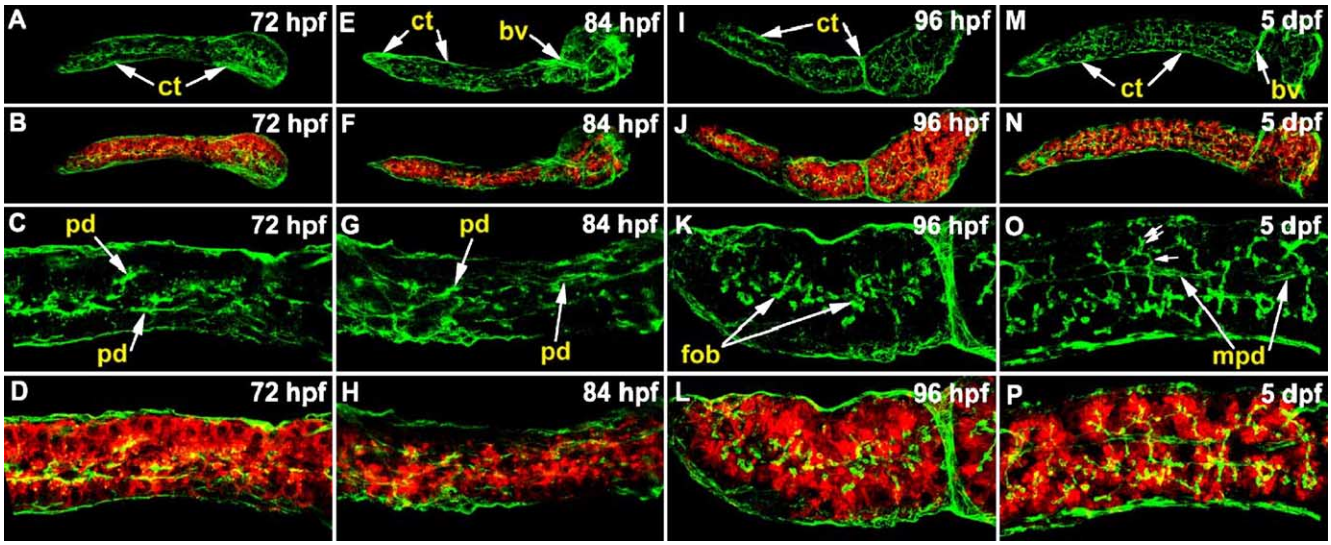

Fig. 4. Pancreatic ductal morphogenesis during larval development. (A–P) Confocal images (right, lateral view) of whole mount specimens processed for cyk (green) and cpa (red) immunohistochemistry. (A–D) At 72 hpf, small primary pancreatic ducts are evident, and there is strong cpa staining in acinar cells. (E–H) The 84 hpf pancreas has a few more ducts than at earlier stages. (I–L) At 96 hpf, first order ductal branches are evident. These small ducts appear to extend into the nearby acinar glands. (M–P) At 120 hpf (5 dpf), second order ductal branches (double arrows) that clearly extend into well formed acini are evident. First order ductal branches (single arrow) and main pancreatic duct segments are also evident at this stage. cyk: cytokeratin; cpa: carboxypeptidase A; pd: pancreatic ducts; fob: first order ductal branches; mpd: main pancreatic duct; ct: connective tissue; bv: blood vessel.

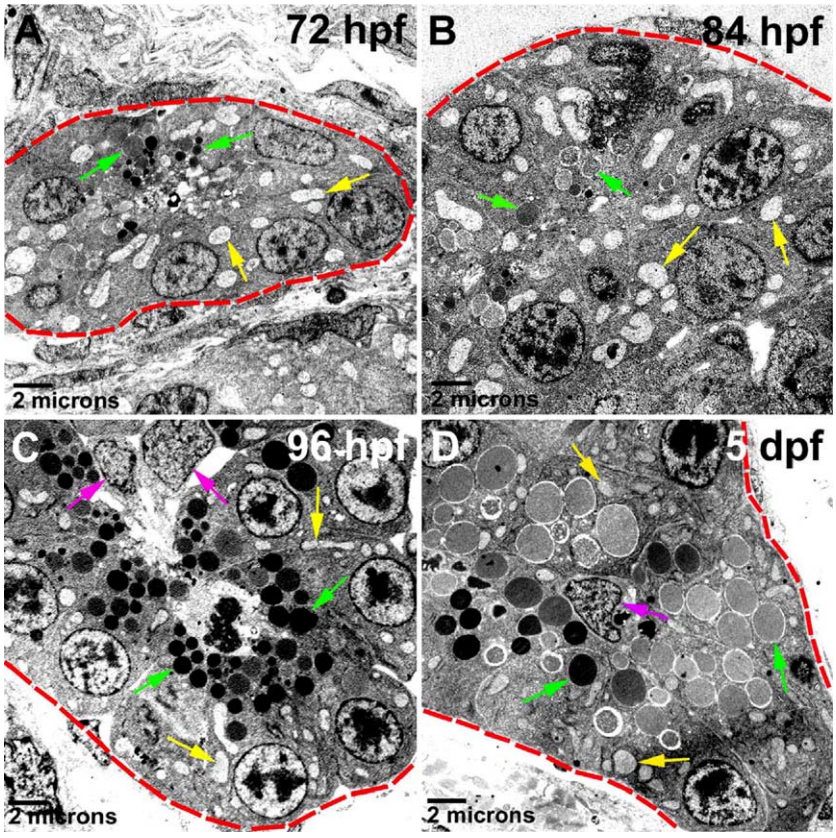

Fig. 5. Acinar cell ultrastructure. (A–D) Transmission electron micrographs of pancreatic acini (outlined by red dashed lines). Progressive maturation of acinar cells is evident between 72 hpf and 5 dpf as determined by the cell polarity, number and size of zymogen granules (green arrows) and the amount of mitochondria (yellow arrows) and rough endoplasmic reticulum. Centroacinar cells are indicated by pink arrows.

To explore this possibility, we treated zebrafish embryos with ethanol, which impedes midline migration of endodermal cells in zebrafish gastrulae (Blader and Strahle, 1998). Embryos treated with ethanol during gastrulation had exocrine pancreas duplications consisting of cpa+ (Fig. 7), *trypsin*+ (not shown) cells and a morphologically identifiable extrapancreatic duct (Fig. 7). However, neither of the duplicated pancreatic ducts inserted into the intestine (Fig. 7). These findings are most compatible with in situ differentiation of bilateral sets of acinar and ductular progenitors (whose midline migration was delayed by ethanol treatment) rather than the formation of duplicate buds that arise and subsequently dissociate from the gut tube. By analogy, these data support the idea that, during normal development, the exocrine anlage arises from bilateral sets of progenitors within the blastoderm margin that migrate to the midline (Warga and Nusslein-Volhard, 1999), fuse and differentiate prior to joining the rostral intestine (gut tube).

Coordinated morphogenesis of the ductular system and acinar glands

Identification of cpa+ and cyk+ cells before the appearance of well defined acinar glands and ducts suggests that pancreatic morphogenetic programs begin after initiation of cellular differentiation. When acinar glands and ducts first form, they do so in close proximity to one another. This further suggests that gland and duct morphogenesis may be directed by common molecular programs. To explore this possibility, we analyzed duct morphology in zebrafish larvae carrying mutations that disrupt acinar development. These mutants were derived from two morphology-based screens (Chen et al., 1996; Pack et al., 1996) and the screening of a smaller collection of mutagenized fish for mutations that altered patterns of immunoreactive cpa and insulin.

The intestinal epithelium and exocrine pancreas of *slimjim* (*slj*^{m74}) and *piebald* (*pie*^{m497}) mutants undergo degeneration between 4 dpf and 5 dpf (Pack et al., 1996). The *flotte lotte* (*flo*^{ti262c}) mutant (Chen et al., 1996) has similar intestinal (Wallace et al., 2005) and exocrine pancreas defects as *slj* and *pie* (Fig. 8). Development of the pancreatic islet occurs normally in each of these mutants (data not shown). Cpa and cyk immunostaining of 4 dpf *slj*, *pie* and *flo* mutants revealed an extrapancreatic duct and a small exocrine remnant that contained virtually no cpa+ cells (Fig. 8). Histological sections of these specimens showed that acinar gland and intrapancreatic duct morphology are severely altered. The 4 dpf cyk staining patterns resembled those of less mature wild type larvae, suggesting that duct development is arrested in each mutant. Supporting this,

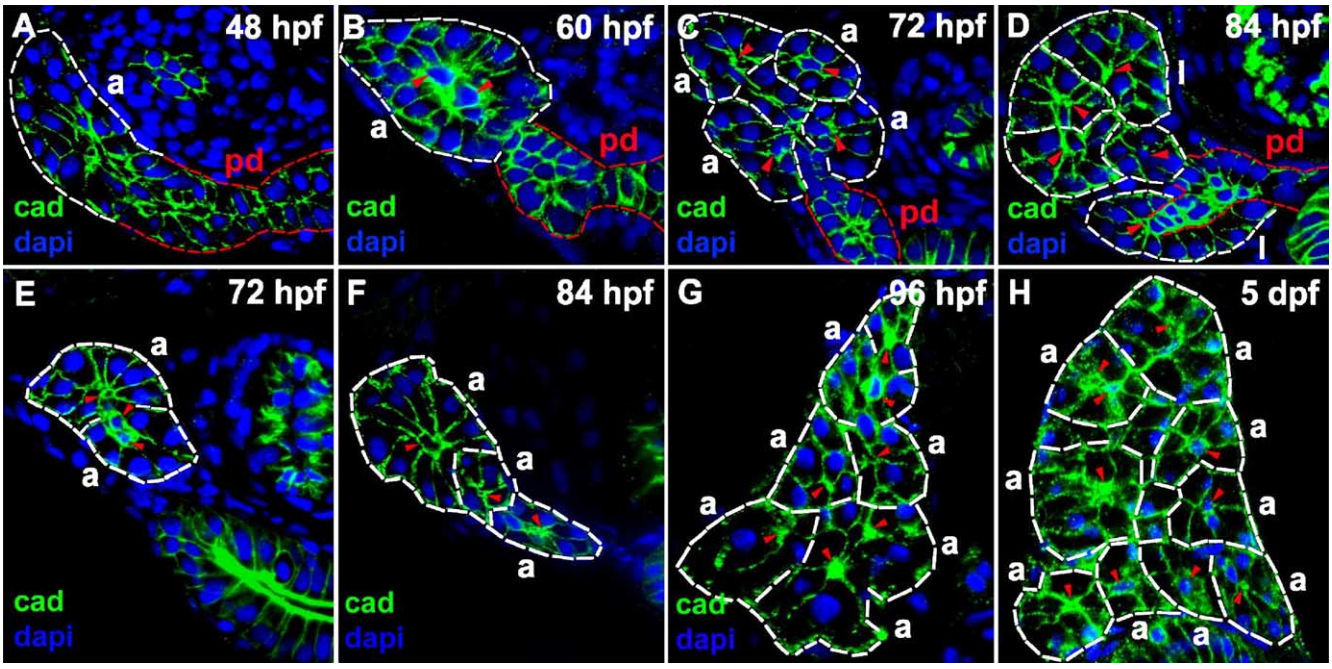

Fig. 6. Acinar gland morphogenesis during larval development. (A–D) Histological sections through the anterior pancreas (rostral to islet) of larvae processed for cadherin (green) immunohistochemistry and dapi (blue). The main pancreatic duct and the acini are demarcated (red and white dashed lines respectively), and centroacinar cells are indicated (red arrowheads). (A) At 48 hpf, the distal end of the main pancreatic duct appears as a multi-layered stratified epithelium (white dashed lines). (B) By 60 hpf, a primitive acinus-like structure is formed. (C) At 72 hpf, four distinct acini are recognized. (D) By 84 hpf, two exocrine lobules are evident. (E–H) Histological cross-sections through the pancreas (caudal to islet) of larvae processed for cadherin immunohistochemistry (green) and dapi (blue). Acini (demarcated by white dashed lines) are shown. Acinar number increases on successive days post-fertilization. Two, three, six and nine acini are identified in these 72 hpf (E), 84 hpf (F), 96 hpf (G) and 5 dpf (120 hpf) (H) larvae, respectively. pd: pancreatic duct; a: acinus; l: exocrine lobule; cad: cadherin.

exocrine size in the *slj*, *pie* and *flo* larvae, as assessed by the expression of *trypsin* (Supplementary Fig. 2) and *ptf1a* (data not shown), was markedly reduced at 72 hpf, whereas it is normal at 48 hpf (data not shown).

Taken together, these data suggest that the functions of the *slj*, *pie* and *flo* genes are required for the proliferation and survival of acinar and ductal progenitors. Compound exocrine defects in these mutants support the hypothesis that acinar and duct development may be regulated by common genetic pathways. To further test this hypothesis, we analyzed four novel exocrine mutants that were identified by altered cpa staining and normal islet morphology. Each mutation is inherited in a Mendelian recessive manner. Complementation studies showed that the mutations affect four distinct genes. Immunohistochemical analyses revealed that these mutations have variable effects on exocrine growth and acinar cytodifferentiation and morphogenesis. Ductular development is also altered by each mutation. However, unlike *slj*, *pie* and *flo*, ductular and acinar defects are not always proportional.

Table 2
Timing of zebrafish exocrine pancreas development

	36 hpf	48 hpf	60 hpf	72 hpf	84 hpf	96 hpf	120 hpf
EPD	+						
CYK		+					
Trypsin		+					
CPA/AMY			+				
Acinus				+			
CAC				+			
Lobule					+		
FOB						+	
SOB							+

EPD: extrapancreatic duct; CYK: cytokeratin protein; trypsin RNA; CPA: carboxypeptidase A protein; AMY: amylase protein; CAC: centroacinar cell; FOB: first order ductal branch; SOB: second order ductal branch; hpf: hour-post-fertilization. "+" indicates initial appearance.

The *sweetbread* (*swd*) mutation affects pancreas and melanophore development. The exocrine pancreas of 5 dpf *swd* mutants is small, and the skin pigmentation is reduced (Figs. 9B1–B4). The *swd* mutants also have reduced numbers of *dopachrome tautomerase* positive (*dct*+) melanoblasts (data not shown), but normal retinal pigmentation (Fig. 9B1). The number and distribution of Hu+ enteric neurons (data not shown) are also normal in *swd* mutants. These findings suggest that the *swd* mutation may affect the development of specific neural crest derivatives. The *swd* phenotype is, to our knowledge, the first that links exocrine pancreas with neural crest development.

Cyk and cpa immunostainings of 5 dpf *swd* mutants revealed reduced branching of intrapancreatic ducts and a marked reduction in the number of acinar cells (Figs. 9B4–B6). The ducts in the *swd* mutant appear to join to form a main duct within the pancreatic tail. A small number of first

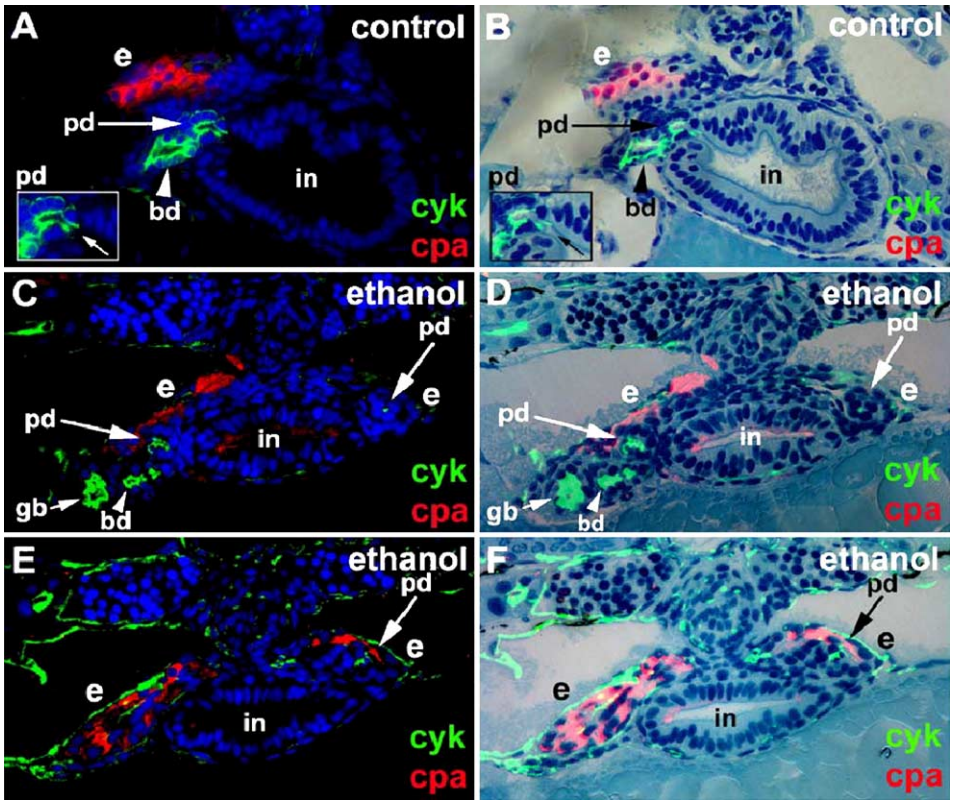

Fig. 7. Ethanol treatment disrupts exocrine pancreas morphogenesis. Histological cross-sections (viewing posteriorly) of a 4 dpf control (A, B) and an ethanol-treated larva (C–F) processed for cyk (green) and cpa (red) immunohistochemistry. (A, C, E) Fluorescent images with dapi (blue); (B, D, F) merged fluorescent images without dapi and bright field images of the corresponding histological sections stained with methylene blue and azure II. (A, B) The extrapancreatic duct and extra-hepatic bile duct of control larvae join the intestine at the same level. Inset shows site of pancreatic duct insertion into the intestine (arrow). (C–F) Bilateral cyk+ and cpa+ exocrine tissues are present in ethanol-treated larva. Bilateral extrapancreatic ducts that fail to join the intestine in these sections, as well as in consecutive rostral and caudal sections (not shown). Sections depicted in panels (C), (D) and (E), (F) are separated by 9 μm (C and D rostral to E and F). cyk: cytokeratin; cpa: carboxypeptidase A; pd: pancreatic duct; bd: bile duct; in: intestine; e: exocrine tissues; gb: gall bladder.

order duct branches were seen in some *swd* mutants (data not shown). Cadherin immunohistochemistry (data not shown) and ultrastructural analysis show that the *swd* exocrine pancreas is comprised of small acini formed by immature exocrine cells (Supplementary Figs. 3C and D). The overall appearance of the 5 dpf *swd* exocrine pancreas resembles a stage intermediate between the 72 hpf and 96 hpf wild type pancreas. Consistent with this idea, exocrine pancreas morphology and size, as assessed with the exocrine markers *trypsin* (Supplementary Figs. 3A and B) and *ptf1a* (data not shown), are both normal in 72 hpf *swd* mutants. We interpret these findings as evidence that the *swd* mutation arrests proliferation of acinar and ductal progenitors. *Swd* mutants are distinguished from *slj*, *pie* and *flo* mutants, which also have arrested development of exocrine progenitors, by their normal pattern of *trypsin* expression at 72 hpf, identifiable cpa+ cells, a larger number of cyk+ ducts and the lack of subsequent degeneration of exocrine cells.

Three other mutations cause distinct patterns of altered ductal branching associated with impaired acinar cell cytodifferentiation. In the *mitomess* (*mms*) mutant, first order ductal branches are evident (Figs. 9C5 and C6). Acinar cells are arranged in glands but have low levels of cpa and zymogen granules (Figs. 9C2, C4 and C6). Prominent cytoplasmic vacuole-like structures are seen in many acinar cells; electron micrographs identified that these vacuoles are dilated mitochondria (Supplementary Figs. 3E–H). The 5 dpf *mms* and *swd* mutants resemble one another in that the pancreas is comprised of incompletely differentiated acinar cells and a truncated ductular network in both mutants. Exocrine morphology and differentiation, as assessed by *trypsin* and *ptf1a* expression (data not shown), are also normal in each mutant at 72 hpf. However, *mms* mutants have first order ductal branches, while such branching is rarely observed in *swd* mutants. Furthermore, compared with *swd*, *mms* larvae have comparatively well-developed acini, but paradoxically, far less cpa protein. Thus, although acinar and duct development are disrupted in both mutants, the relative defects in each lineage are disproportional.

Acinar and ductular defects in two other exocrine mutants, *ductjam* (*djm*) and *ducttrip* (*dtp*), are distinguishable from *swd* and *mms* mutants. In *djm* larvae, segments of the main intrapancreatic duct, when visible, are truncated, and they appear ectatic as do the few identifiable ductal

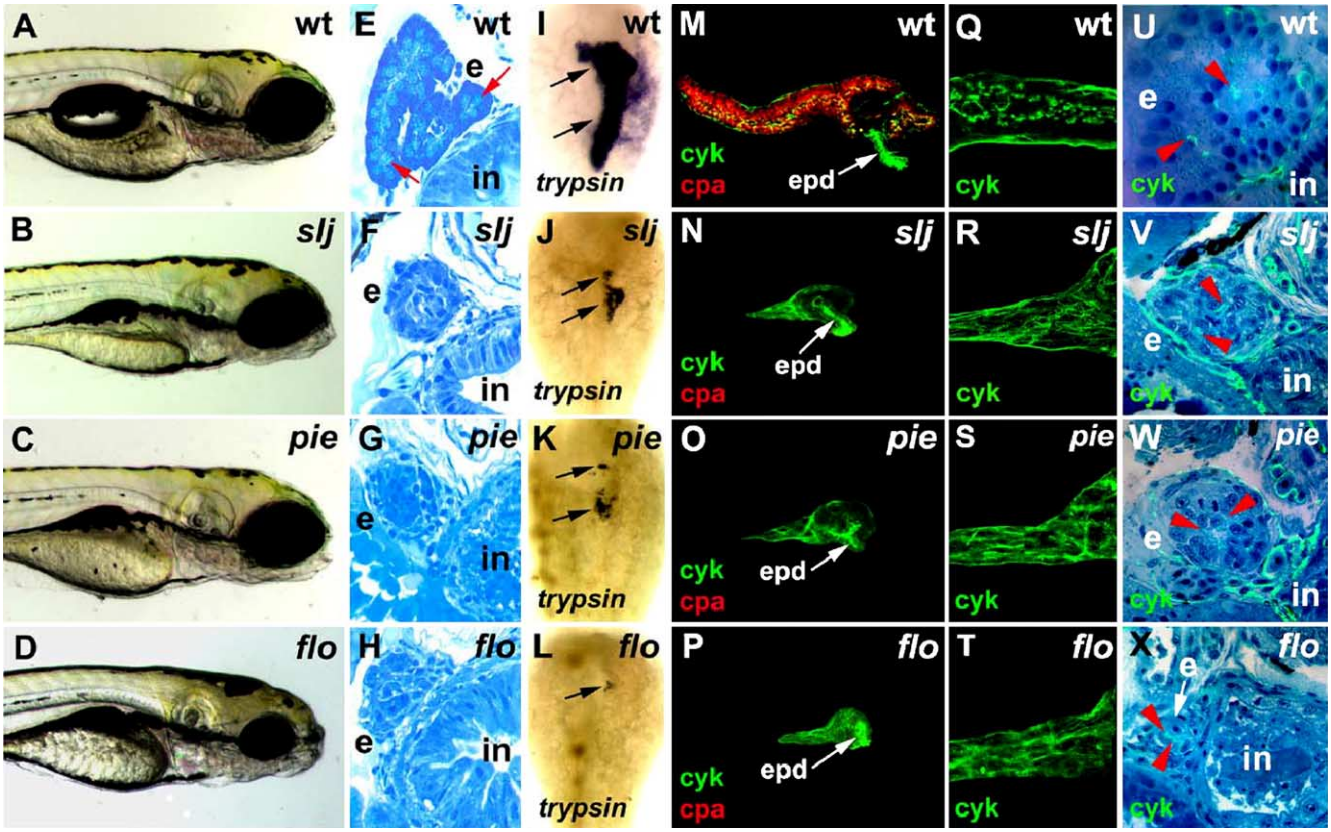

Fig. 8. Mutations affecting early stages of exocrine pancreas development on 4 dpf. Right lateral view of live wild type (A), *slj* (B), *pie* (C) and *flo* (D) larvae. In the wild type larva (A), the intestinal epithelium is folded, only a small amount of yolk is evident, and the swim bladder is inflated. By comparison, the intestines in *slj* (B), *pie* (C) and *flo* (D) are narrow, and they lack folds. (E–H) Histological cross-sections through the exocrine pancreas 3 μm caudal to the islet. Wild type acinar cells contain zymogen granules (E, red arrows), whereas in *slj* (F), *pie* (G) and *flo* (H), the pancreatic cells lack zymogen granules. (I–L) Dorsal view of larvae processed for whole mount RNA in situ hybridization using an antisense *trypsin* probe. Strong *trypsin* expression is present in the wild type larva (I), whereas in *slj* (J), *pie* (K) and *flo* (L) larvae, there is reduced *trypsin* expression. Arrows point at pancreatic head and pancreatic tail. (M–P) Wild type and mutant pancreata processed for whole mount cyk and cpa immunohistochemistry (IHC). The wild type exocrine pancreas (M) is comprised of cpa+ acinar cells and a network of cyk+ ducts that joins the extrapancreatic main duct. The exocrine pancreata of *slj* (N), *pie* (O) and *flo* (P) larvae are small. The extrapancreatic duct can be identified, but there is no significant cpa detected, and only a small number of ducts are recognizable. (Q–T) Confocal analysis of pancreatic ducts following cyk IHC. Ducts in the mutant pancreata resemble primary ducts seen in wild type larvae (Figs. 4C, G). (U–X) Histological cross-sections through the pancreas ~3 μm posterior to the islet of larvae processed for cyk IHC merged with bright field images of the corresponding histological sections stained with methylene blue and azure II. Small ducts are evident in the wild type larva (U; arrowheads) and in *slj* (V), *pie* (W) and *flo* (X) larvae). *slj*: *slimjim*; *pie*: *piebald*; *flo*: *flotte lotte*; e: exocrine pancreas; in: intestine; cyk: cytokeratin; cpa: carboxypeptidase A; epd: extrapancreatic main duct.

branches (Figs. 9D4–D6). In *dtp* larvae, only small duct remnants are present (Figs. 9E4–E6). Histological analyses of both mutants processed for cyk immunohistochemistry showed that some of the cyk+ cells had arranged as small ducts (data not shown). Acinar cells in both mutants were markedly reduced in number, poorly organized and rarely, weakly cpa+ (Figs. 9D4 and D6, E4 and E6). As described for *mms* and *swd* mutants, normal *trypsin* and *ptf1a* expression patterns were present within the pancreas of 72 hpf *djm* mutants (data not shown). By contrast, 72 hpf *dtp* mutant larvae had normal numbers of *trypsin*+ cells, but levels of *trypsin* expression were reduced compared with wild type siblings (Supplementary Fig. 2E). These findings distinguish early stage (72 hpf) *djm* and *dtp* mutants from *slj*, *pie* and *flo*, whereas the ductal anatomy of both groups of mutants is quite similar (Supplementary Fig. 2, Figs. 8 and 9).

A phenotypic comparison of the seven exocrine pancreas mutants is presented in Table 3.

Notch signaling preferentially regulates pancreatic duct development in zebrafish larvae

Pancreas mutants described in this report were identified using organ morphology or cpa staining patterns as screening criteria. With this strategy, mutants that have both acinar and duct defects were recovered, whereas mutants with isolated ductal defects may have been overlooked. Recently, we have shown that pancreatic duct development is selectively altered by targeting of *jagged*-mediated Notch signaling; compound knockdowns of zebrafish *jagged2* and *jagged3* genes lead to the formation of enlarged acini and a paucity of ducts within the pancreatic parenchyma (Lorent et al., 2004). Here, we

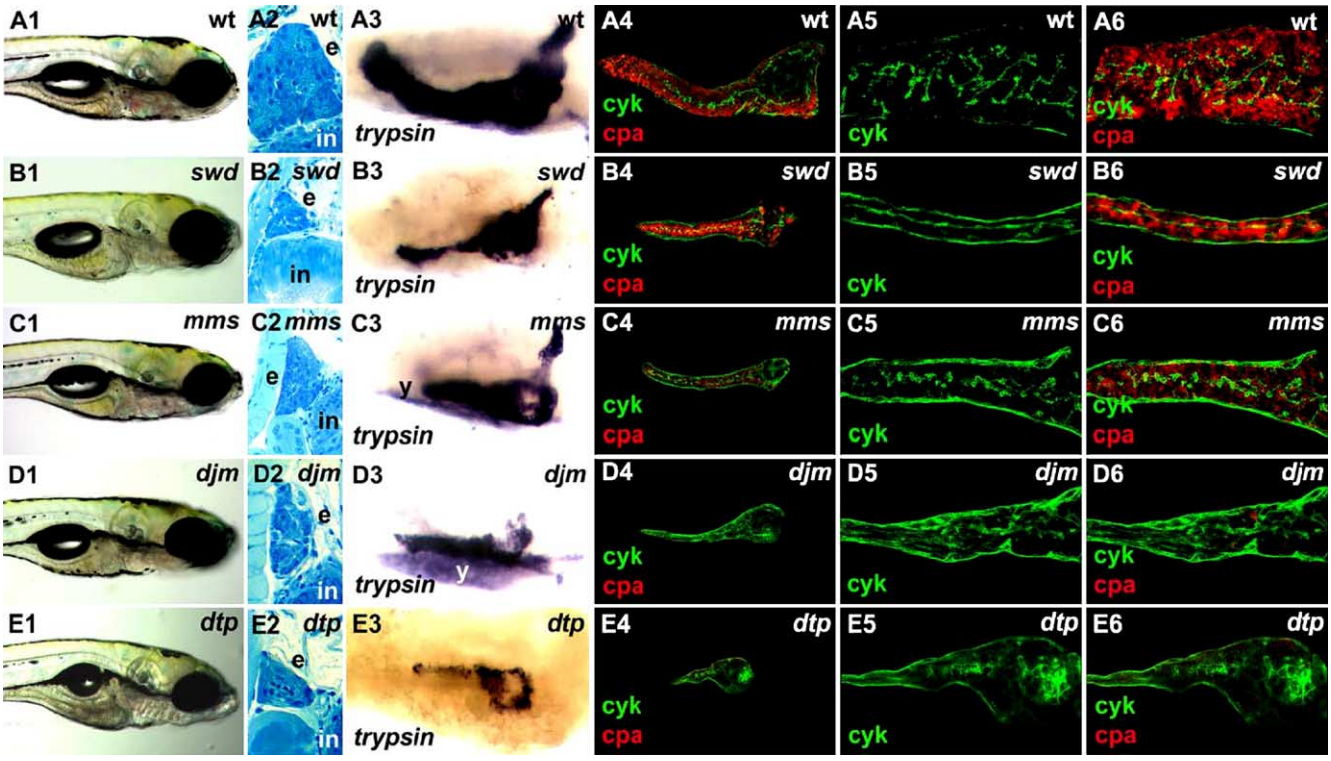

Fig. 9. Mutations affecting late stages of exocrine pancreas development. (A1–E1) Right lateral view of live 5 dpf wild type and mutant larvae. (A1) The wild type intestinal epithelium is folded, a widely patent gut lumen is obvious, and there is little residual yolk. The intestine is grossly normal in *swd* (B1), *mms* (C1), *djm* (D1) and *dtp* (E1) mutants. In *swd*, skin pigmentation (melanophores) is reduced, but xanthophores and iridophores appear unaffected (B1). There is a small amount of residual yolk in *dtp* (E1). (A2–E2) Histological cross-sections through the 5 dpf pancreas, 3 μm caudal to the islet. In wild type (A2), there are multiple exocrine acini; in *swd* (B2), there are relatively few exocrine acini, and electron micrograph shows that the acinar cells contain zymogen granules (Supplementary Fig. 3D); in *mms* (C2), multiple acini are observed, but the cytoplasm of the acinar cells contains vacuole-like structures and very few zymogen granules (Supplementary Fig. 3H); in *djm* (D2) and *dtp* (E2), there are no recognizable acini present, and the exocrine cells appear undifferentiated. (A3–E3) Right lateral view of whole mount *trypsin* in situ hybridization on 5 dpf. Strong *trypsin* expression is evident in the wild type pancreas (A3), whereas in *swd* (B3), *mms* (C3), *djm* (D3) and *dtp* (E3), *trypsin* expression is reduced. There is background staining in the yolk. (A4–E4) Visualization of pancreatic ducts and acinar cells by cyk and cpa immunohistochemistry, respectively. The wild type ductal system is composed of a branching network of small ducts and cpa+ acinar cells (A4). The *swd* pancreas (B4) is small, but there is relatively normal cpa; in the *mms* pancreas (C4), there are only low levels of cpa. There is no significant cpa detected in *djm* (D4) and *dtp* (E4). (A5–E5 and A6–E6) Confocal projection of pancreatic ducts (green) and acini (red) in larvae processed for cyk and cpa immunohistochemistry. Wild type pancreatic ducts are highly branched, and individual acini are each drained by single intercalated duct (A5, 6). In *swd* (B5, 6), the main pancreatic duct with few branches is evident, whereas in *mms* (C5, 6), duct branching is evident, albeit less pronounced than in wild type. By comparison, the ductal networks of *djm* (D5, 6) and *dtp* (E5, 6) are markedly aberrant. *swd*: *sweetbread*; *mms*: *mitomess*; *djm*: *ductjam*; *dtp*: *ducttrip*; e: exocrine pancreas; in: intestine; y: yolk; cyk: cytokeratin; cpa: carboxypeptidase A.

present a more detailed examination of the pancreatic phenotype of these and other larvae in which Notch signaling is altered.

Histological analyses of cpa/cyk immunostained *jagged2/3* morpholino-injected larvae revealed that the enlarged acini observed in whole mount specimens were contiguous and their lumens formed elongated duct-like structures (Figs. 10A–D). These studies also confirmed the presence of apical acinar cell cyk protein as suggested by confocal analyses (Lorent et al., 2004). Ultrastructural analyses of *jagged2/3* morpholino-injected larvae confirmed the presence of enlarged acinar glands comprised of normally differentiated exocrine cells (Figs. 10E and F). Centroacinar cells were absent, and ducts were not identified (Table 3).

Consistent with these findings, zebrafish *mind bomb* (*mib*^{m132}) mutants, which are deficient in the function of a ubiquitin ligase that is essential for Delta- (Itoh et al., 2003) and possibly Jagged-mediated Notch signaling (A. Chitnis, personal communication) had related exocrine defects. Previous studies have shown precocious expression of the exocrine markers *ptf1a* and *trypsin* in *mib* mutants (Esni et al., 2004). Here, we show that duct development is disrupted by the *mib* mutation. Cpa and cyk immunohistochemistry showed that 5 dpf *mib* larvae have paucity of intrapancreatic ducts and enlarged acini that resemble the acini of *jagged2/3* morpholino-injected larvae (Figs. 10G and B, Table 3). Histological analysis confirmed these findings (Figs. 10I and J). Exocrine development was less advanced in *mib* larvae than in *jagged2/3* morpholino-injected larvae, a difference we attribute to the general delay in larval development associated with loss of *mib* gene function.

Table 3
Summary of exocrine pancreas features of zebrafish mutations

	slj	*pie*	*flo*	*swd*	*mms*	*djm*	*dtp*	*jag*-MO	*mib*	*notch1a-ICD*
EPD	+	+	+	+	+	+	+	+	+	+
PRD	+/−	+/−	+/−	+	+	+/−	+/−	+/−	+/−	+
FOB	−	−	−	+/−	+	−	−	−	−	−
SOB	−	−	−	−	−	−	−	−	−	−
CAC	−	−	−	+	+	−	−	−	−	+
Acinus	−	−	−	+	+	−	−	+	+	+
CPA/AMY	−	−	−	+	+	−	−	+	+	+

slj: *slimjim*; *pie*: *piebald*; *flo*: *flotte lotte*; *swd*: *sweetbread*; *mms*: *mitomess*; *djm*: *ductjam*; *dtp*: *ducttrip*; *jag*-MO: *jagged2/3 morphant*; *mib*: *mind bomb*; *notch1a-ICD*: *notch1a-intracellular domain*.
EPD: extrapancreatic duct; PRD: primary ducts; FOB: first order ductal branch; SOB: second order ductal branch; CAC: centroacinar cell; CPA: carboxypeptidase A protein; AMY: amylase protein. "+" indicates presence; "+/−" indicates variable or reduced presence; "−" indicates absence.

One way of explaining the combination of precocious acinar differentiation and ductal paucity in Notch-deficient larvae is to postulate that the Notch signal normally maintains larval exocrine progenitors in an undifferentiated state and that, upon loss of this signal progenitor, cells adopt a default acinar rather than duct cell fate. Notch has been proposed to play such a suppressive role in the developing mammalian pancreas, although here the default fate is endocrine rather than exocrine (Apelqvist et al., 1999; Jensen et al., 2000). Alternatively, it could be argued that, in zebrafish, Notch directly promotes duct development, and that in Notch-deficient larvae, acinar development, albeit premature, is otherwise unaffected. Notch activation experiments could theoretically help distinguish between these two models of how Notch regulates duct development; the former predicts that Notch activation should inhibit duct development, while the latter predicts that Notch activation should promote duct development.

Previous work has shown that delayed *trypsin* gene expression occurs following Notch activation in early zebrafish embryos (Esni et al., 2004). Duct development could not be assessed in these Notch-activated fish at larval stages because of developmental delays (data not shown). For this reason, we analyzed larvae in which Notch activation was initiated at later developmental time points. Larvae induced to express a constitutively active *notch1a-ICD* transgene beginning at 72 hpf developed in a near normal fashion but had exocrine defects. Acinar differentiation, as determined by cpa immunostaining, appeared normal in most larvae (Fig. 10H; n = 18 of 20 larvae) but was altered in others, as evidenced by reduced levels of cpa protein and small zymogen granules (data not shown). Importantly, the ductal system was truncated in all of the Notch-activated larvae and in none of these larvae were ectopic pancreatic ducts identified (Fig. 10H, Table 3). These findings argue against a direct role for the Notch signal in duct development and instead support a model in which Notch normally functions to maintain undifferentiated exocrine progenitors.

Discussion

Although a significant number of genes that regulate endocrine pancreas development have been identified, relatively few genes are known to play a specific role in development of the exocrine pancreas. Furthermore, very little is known about the developmental biology of this organ. In this report, we characterize zebrafish exocrine anatomy and development and describe mutations that perturb exocrine development in larval zebrafish.

Stages of exocrine development: 1. Formation of the exocrine anlage and appearance of protodifferentiated progenitor cells

Immunohistochemical and ultrastructural analyses of wild type embryos and larvae allow us to define two stages of exocrine pancreas organogenesis. During the first stage of exocrine development, *ptf1a*+ progenitor cells appear within endoderm rostral to and within a small number of cells of the newly formed gut tube (Lin et al., 2004; Zecchin et al., 2004). At this stage, presumptive exocrine progenitor cells also express the homeobox transcription factor *mnr2a* (Wendik et al., 2004). Later, these cells migrate to surround the solitary pancreatic islet. The *ptf1a*+ progenitors within the exocrine anlage begin to express the acinar gene *trypsin* but lack histological features of differentiated cells and do not contain digestive enzyme proteins such as cpa and amylase (unpublished data) or the cytokeratin duct marker. Thus, we consider these cells protodifferentiated exocrine progenitors.

This first phase of zebrafish exocrine development may be considered analogous to the stage of mammalian pancreas development when ventral and dorsal pancreatic anlagen form. Function of both *ptf1a* and *pdx1* genes are required for this stage of exocrine development in zebrafish and mammals (Jonsson et al., 1994; Kawaguchi et al., 2002; Krapp et al., 1998; Lin et al., 2004; Offield et al., 1996; Yee et al., 2001; Zecchin et al., 2004). These similarities notwithstanding, we show that the zebrafish exocrine anlage forms and is arranged in a different fashion than its mammalian counterparts. The mammalian pancreatic anlagen are comprised of undifferentiated progenitor cells arranged in a single-layered folded epithelium that is contiguous with the gut tube. The epithelium is also surrounded by a thick layer of mesenchymal cells. By contrast, progenitor cells within the zebrafish exocrine anlage are arranged in a stratified epithelium. A pronounced mesenchymal layer surrounding the exocrine progenitors is not identified. Furthermore, zebrafish exocrine progenitors appear to arise from endoderm rostral to the gut tube, which it subsequently joins, rather than as an extension of the epithelium of the main duct. Thus, we argue against a classical model (Field et al., 2003) in which the zebrafish exocrine pancreas buds from either a rod of pre-intestinal endoderm or the gut tube which in zebrafish gives rise to the

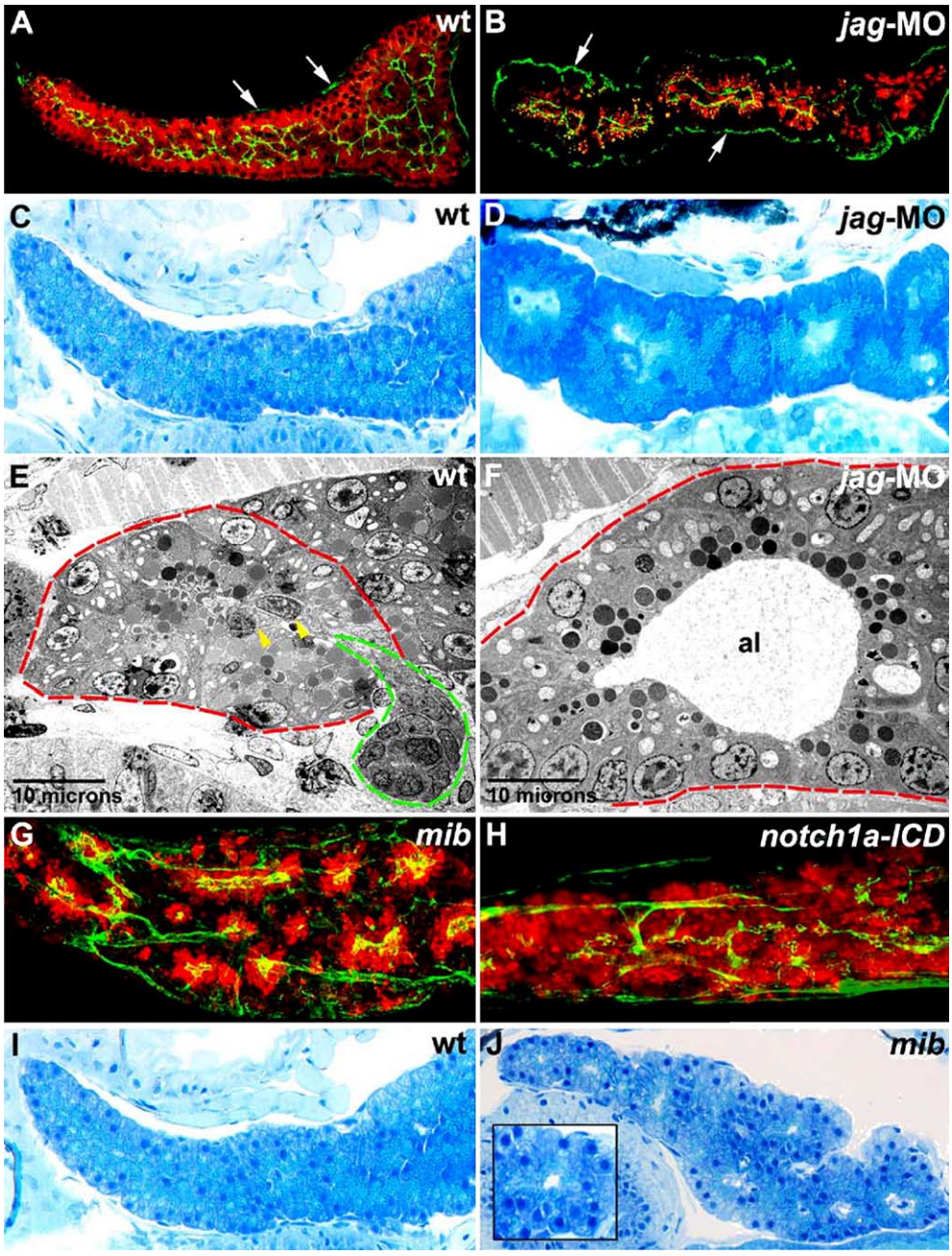

Fig. 10. Notch signaling regulates pancreatic duct development. (A, B) Sagittal optical section (A) and histological section (B) of the pancreas of wild type (A) and *jagged2/3* morpholino-injected (B) 5 dpf larvae processed for cpa (red) and cyk (green) immunohistochemistry (IHC), right lateral view. Cpa is present in the *jagged* morpholino-injected larva (B), although the levels are reduced compared with wild type (A). By contrast, the ductal system is markedly reduced in the *jagged* morpholino-injected larva (B). (C, D) Sagittal histological sections through the pancreas of 5 dpf wild type (C) and *jagged* morpholino-injected (D) larvae. Note the contiguous enlarged acini present in the *jagged* morpholino-injected larva. By contrast, individual wild type acini are difficult to delineate because they are numerous, relatively small and in close proximity to each other. (E, F) Transmission electron micrographs showing acini (red dashed lines) from wild type (E) and *jagged* morpholino-injected (F) larvae. The acinar lumen of the *jagged* morpholino-injected larva is dilated, and centroacinar cells are absent. An intercalated duct exiting the wild type acinus is evident (green dashed line), and two centroacinar cells are indicated by yellow arrowheads. (G, H) Confocal projection of larvae processed for cyk (green) and cpa (red) IHC. Cyk IHC shows altered ductal morphology in *mib* (G) and Notch-activated (H) larvae. Cpa IHC shows clusters of enlarged acini in *mib* (G), whereas following Notch activation, the level and distribution of cpa protein are near normal (H), compared with wild type pancreas (Figs. 4O and P; Figs. 9A5 and A6). (I, J) Sagittal histological sections through the 5 dpf wild type (I) and *mib* (J) pancreas, right lateral view. Note enlarged acini (inset showing a magnified view) in the *mib* larva. *jag*-MO: *jagged2/3* morphant; *mib*: *mind bomb*; *notch1a-ICD*: *notch1a-intracellular domain*; cpa: carboxypeptidase A; cyk: cytokeratin; al: acinar lumen. Arrows in panels (A) and (B) point to immunoreactive cyk in pancreatic connective tissue.

intestine (Wallace and Pack, 2003). A previous study defining the zebrafish endodermal fate map seems to support our model in that only one of six singly labeled blastomeres within the zebrafish embryo that gave rise to pancreas also gave rise to intestine (Warga and Nusslein-Volhard, 1999). However, formal resolution of these models

may not be feasible without a more detailed lineage analysis.

Stages of exocrine development: 2. Exocrine differentiation and acinar gland and duct morphogenesis

Acinar and duct cytodifferentiation and morphogenesis define the second stage of exocrine development. During this phase, the onset of cytodifferentiation precedes gland and duct morphogenesis in the region surrounding the islet. Here, and at slightly later stages in the pancreatic tail, differentiated cpa+ and cyk+ cells appear to arise contemporaneously. The ductular system appears to arise from the cyk+ cells in situ, in the form of small networks that ultimately join to form a contiguous structure. This model of duct morphogenesis in zebrafish contrasts with the classical branching morphogenesis model of mammalian exocrine duct formation, but it resembles the mechanism of duct formation in developing salivary and mammary glands (Hieda et al., 1996; Hogg et al., 1983). Interestingly, in over half of the larvae we analyzed, ducts draining adjacent acini appeared linked directly to one another rather than to a well defined main pancreatic duct. In the remaining larvae, acini within short segments drained into a common, albeit segmented main duct that did not directly link to comparable ducts within adjacent segments. This ductal morphology may not be surprising, given the highly branched, and thus diffuse architecture of the mature pancreas of adult fish.

In addition to duct formation, acinar gland morphogenesis was also evident during the second stage of zebrafish exocrine pancreas development. Well-formed acini and small ducts were clearly evident in 72 hpf larvae, a time point beyond when cpa and cyk protein, markers of differentiated acinar and duct cells, were first evident. The number of ducts and acini increased considerably during subsequent stages of larval development. Although we can only speculate as to the mechanism of acinar expansion, our impression from BrdU immunostaining (unpublished data) is that new acinar glands arise, at least in part through proliferation of differentiated (cpa+) acinar cells. Whether expansion of the ductal system also involves proliferation of differentiated cells could not be addressed because of the difficulty encountered identifying duct nuclei in histological sections.

Distinct pancreatic phenotypes arise from mutations affecting early and late stages of exocrine development

Mutations affecting exocrine pancreas and intestinal development were described in previous morphology-based mutagenesis screens (Pack et al., 1996). Here, we show that two of these mutants (*slj* and *pie*) and a third intestinal mutant not previously known to alter pancreas development (*flo*) (Chen et al., 1996) have related exocrine phenotypes. All three mutations affect expansion of the exocrine anlage during the initial phase of exocrine development. In these mutants, there is also a general failure of exocrine cytodifferentiation, and gland and duct morphogenesis followed by cellular degeneration. These phenotypic features, coupled with intestinal (Wallace et al., 2005) and pharyngeal defects (not shown) of these mutants, suggest that the responsible genes regulate pathways required for the maintenance of digestive epithelia. Thus, it may not be surprising that these mutants had pronounced acinar and duct defects. Whether these mutations interfere with genes that have been shown to be essential for mesenchymal-mediated expansion of the mammalian pancreas anlagen, such as *fgf10* (Bhushan et al., 2001), *isl1* (Ahlgren et al., 1997) or *N-cadherin* (Esni et al., 2001), may be explored in subsequent studies.

Four novel exocrine mutants identified by the presence of reduced cpa staining but comparatively normal intestinal morphology are also described in this report. Normal or near-normal *trypsin* expression patterns in each mutant at 72 hpf suggest that the affected genes regulate the second phase of pancreas organogenesis. Although the appearances of these mutant pancreata are similar at this stage, histological and immunohistochemical analyses at subsequent stages revealed variable acinar and duct defects. For example, acinar and ductal differentiation and morphogenesis appeared to be disproportionately delayed in *swd* mutants and *mms* mutants. By contrast, pronounced acinar and ductal defects were seen in *djm* and *dtp* mutants. Thus, variable defects may arise from mutations that appear to affect the second stage of exocrine development.

Pancreatic phenotypes of Notch-deficient and Notch-activated larvae establishes a link between acinar morphogenesis and intrapancreatic duct development

Phenotypic comparison of the pancreas mutants presented in this study suggests that common molecular programs may regulate acinar and duct differentiation and morphogenesis. Analysis of larvae in which the Notch signaling pathway was disrupted allowed us to begin to refine our understanding of this relationship. Notch-deficient *mib* and *jagged2/3* morpholino-injected larvae lack nearly all intrapancreatic ducts but have differentiated acinar cells that are arranged in broad tubules rather than well defined glands. They are distinguished from the previously described pancreas mutants that have strong ductal phenotypes (*slj*, *pie*, *flo*, *dtp* and *djm*) by their highly differentiated acinar cells and their distorted glandular architecture. Exocrine defects in *mib* and *jagged* morpholino-injected larvae suggest that the Notch signal is required for the development of intrapancreatic ducts and proper morphogenesis of the acinar gland, but not acinar cell differentiation.

An interesting aspect of the *mib* and *jagged* knockdown phenotypes is the presence of the cytokeratin duct marker in differentiated acinar cells. The presence of acinar cell cyk supports the idea that the Notch signal regulates ductal

differentiation of a common acinar–duct cell progenitor. We theorize that, in the absence of Notch activity, these progenitors adopt an acinar rather than ductal cell fate. Since ectopic ducts were not identified following Notch activation at larval stages, we also hypothesize that one function of Notch in the developing zebrafish pancreas is to suppress ductal differentiation of bipotential progenitor cells. A related suppressive mechanism of Notch signaling during mammalian pancreas development (Hald et al., 2003; Hart et al., 2003; Murtaugh et al., 2003) has also been proposed to be mediated by Jagged ligands (Norgaard et al., 2003). Similarly, previous work in zebrafish has shown delayed *insulin* and *trypsin* expression following Notch activation at embryonic stages (Esni et al., 2004). Interestingly, this suppressive role of Notch in the zebrafish exocrine pancreas contrasts with its role in the developing zebrafish and mammalian liver. Here, Notch inhibition (Lorent et al., 2004; Piccoli and Spinner, 2001) and activation (B. Stanger and D. Melton, personal communication) have reciprocal effects on bile duct formation.

These arguments notwithstanding, we recognize that there are alternative explanations for the exocrine phenotypes of Notch-deficient and Notch-activated larvae. For example, acinar cyk immunoreactivity in Notch-deficient *mib* and *jagged2/3* morpholino-injected larvae could arise from the transdifferentiation of duct cells or ectopic cyk expression. The well known propensity of mammalian acinar cells to undergo ductular metaplasia (Arias and Bendayan, 1993; Cano et al., 2004; De Lisle and Logsdon, 1990; Hall and Lemoine, 1992; Miyamoto et al., 2003; Pin et al., 2001; Scarpelli et al., 1991) supports this latter hypothesis. Similarly, ductal paucity in Notch-activated larvae, which we argue supports the suppressive model of Notch function, could arise from reduced proliferation or apoptosis of committed duct cells rather than maintenance of ductal progenitors in an undifferentiated state. Future experiments, in which Notch is activated in labeled exocrine progenitors, such as those that express *ptf1a*, may help test these hypotheses.

Conclusion

Genetic analyses in zebrafish offer the opportunity to identify genes that selectively regulate exocrine rather than endocrine pancreas development and physiology. Screens to identify such mutants in zebrafish are feasible because endocrine and exocrine progenitors are segregated at a relatively early developmental stage. In this study, we characterize exocrine development in larval zebrafish and describe mutant phenotypes using two screening strategies. We show mutations that disrupt digestive system morphology likely target progenitor cell function during early stages of exocrine development, whereas mutations that preferentially target exocrine differentiation more likely disrupt later developmental processes. In both sets of mutants, the larval endocrine pancreas developed normally. However, the development of accessory islets that are embedded within adult, but not larval zebrafish exocrine tissue could not be assessed because all mutants die during either larval or early juvenile stages. Thus, it is conceivable that genes that direct exocrine pancreas development in zebrafish larvae also play a role in subsequent stages of endocrine pancreas development.

Acknowledgments

We thank Ajay Chitnis for providing *mind bomb* (*mib*^{m132}) mutant fish, Bruce Appel and Steve Leach for providing *hsp70/GAL4* and *UAS/notch1a-ICD* transgenic fish and the Tubingen zebrafish stock center for *flotte lotte* (*flo*^{ti262c}) mutant fish. This work was supported by National Institutes of Health grants RO1 DK61142 and RO1 DK60369 (M.P.), and KO8 DK60529 (N.S.Y.). Assistance was also provided through the University of Pennsylvania Center for Molecular Studies in Digestive and Liver Disease (NIH P30 DK 50306).

Appendix A. Supplementary data

Supplementary data associated with this article can be found, in the online version, at doi:10.1016/j.ydbio.2005.04.035.

References

Ahlgren, U., Pfaff, S.L., Jessell, T.M., Edlund, T., Edlund, H., 1997. Independent requirement for ISL1 in formation of pancreatic mesenchyme and islet cells. Nature 385, 257–260.

Apelqvist, A., Li, H., Sommer, L., Beatus, P., Anderson, D.J., Honjo, T., Hrabe de Angelis, M., Lendahl, U., Edlund, H., 1999. Notch signaling controls pancreatic cell differentiation. Nature 400, 877–881.

Arias, A.E., Bendayan, M., 1993. Differentiation of pancreatic acinar cells into duct-like cells in vitro. Lab. Invest. 69, 518–530.

Bardeesy, N., DePinho, R.A., 2002. Pancreatic cancer biology and genetics. Nat. Rev., Cancer 2, 897–909.

Bhushan, A., Itoh, N., Kato, S., Thiery, J.P., Czernichow, P., Bellusci, S., Scharfmann, R., 2001. *Fgf10* is essential for maintaining the proliferative capacity of epithelial progenitor cells during early pancreatic organogenesis. Development 128, 5109–5117.

Biemar, F., Argenton, F., Schmidtke, R., Epperlein, S., Peers, B., Driever, W., 2001. Pancreas development in zebrafish: early dispersed appearance of endocrine hormone expressing cells and their convergence to form the definitive islet. Dev. Biol. 230, 189–203.

Blader, P., Strahle, U., 1998. Ethanol impairs migration of the prechordal plate in the zebrafish embryo. Dev. Biol. 201, 185–201.

Cano, D.A., Murcia, N.S., Pazour, G.J., Hebrok, M., 2004. *orpk* mouse model of polycystic kidney disease reveals essential role of primary cilia in pancreatic tissue organization. Development 131, 3457–3467.

Chen, J.N., Haffter, P., Odenthal, J., Vogelsang, E., Brand, M., van Eeden, F.J.M., Furutani-Seiki, M., Granato, M., Hammerschmidt, M., Heisenberg, C.P., Jiang, Y.J., Kane, D.A., Kelsh, R.N., Mullins, M.C., Nusslein-Volhard, C., 1996. Mutations affecting the cardiovas-

cular system and other internal organs in zebrafish. Development 123, 293–302.
De Lisle, R.C., Logsdon, C.D., 1990. Pancreatic acinar cells in culture: expression of acinar and ductal antigens in a growth-related manner. Eur. J. Cell Biol. 51, 64–75.
Dosch, R., Wagner, D.S., Mintzer, K.A., Runke, G., Wiemelt, A.P., Mullins, M.C., 2004. Maternal control of vertebrate development before the midblastula transition: mutants from the zebrafish I. Dev. Cell 6, 771–780.
Esni, F., Johansson, B.R., Radice, G.L., Semb, H., 2001. Dorsal pancreas agenesis in N-cadherin-deficient mice. Dev. Biol. 238, 202–212.
Esni, F., Ghosh, B., Biankin, A.V., Lin, J.W., Albert, M.A., Yu, X., MacDonald, R.J., Civin, C.I., Real, F.X., Pack, M.A., Ball, D.W., Leach, S.D., 2004. Notch inhibits Ptf1 function and acinar cell differentiation in developing mouse and zebrafish pancreas. Development 131, 4213–4224.
Field, H.A., Si Dong, P.D., Beis, D., Stainier, D.Y.R., 2003. Formation of the digestive system in zebrafish. II. Pancreas morphogenesis. Dev. Biol. 261, 197–208.
Gittes, G.K., Galante, P.E., Hanahan, D., Rutter, W.J., Debase, H.T., 1996. Lineage-specific morphogenesis in the developing pancreas: role of mesenchymal factors. Development 122, 439–447.
Gu, G., Dubauskaite, J., Melton, D.A., 2002. Direct evidence for the pancreatic lineage: NGN3+ cells are islet progenitors and are distinct from duct progenitors. Development 129, 2447–2457.
Gu, G., Brown, J.R., Melton, D.A., 2003. Direct lineage tracing reveals the ontogeny of pancreatic cell fates during mouse embryogenesis. Mech. Dev. 120, 35–43.
Hald, J., Hjorth, J.P., German, M.S., Madsen, O.D., Serup, P., Jensen, J., 2003. Activated Notch1 prevents differentiation of pancreatic acinar cells and attenuate endocrine development. Dev. Biol. 260, 426–437.
Hall, P.A., Lemoine, N.R., 1992. Rapid acinar to ductal transdifferentiation in cultured human exocrine pancreas. J. Pathol. 166, 97–103.
Hart, A., Papadopoulou, S., Edlund, H., 2003. Fgf10 maintains notch activation, stimulates proliferation, and blocks differentiation of pancreatic epithelial cells. Dev. Dyn. 228, 185–193.
Hieda, Y., Iwai, K., Morita, T., Nakanishi, Y., 1996. Mouse embryonic submandibular gland epithelium loses its tissue integrity during early branching morphogenesis. Dev. Dyn. 207, 395–403.
Hogan, B.L.M., Kolodziej, P.A., 2002. Molecular mechanisms of tubulogenesis. Nat. Rev., Genet. 3, 513–523.
Hogg, N.A.S., Harrison, C.J., Tickle, C., 1983. Lumen formation in the developing mouse mammary gland. J. Embryol. Exp. Morphol. 73, 39–57.
Holland, A.M., Hale, M.A., Kagami, H., Hammer, R.E., MacDonald, R.J., 2002. Experimental control of pancreatic development and maintenance. Proc. Natl. Acad. Sci. U. S. A. 99, 12236–12241.
Itoh, M., Kim, C.-H., Palardy, G., Oda, T., Jiang, Y.-J., Maust, D., Yeo, S.-Y., Lorick, K., Wright, G.J., Ariza-McNaughton, L., Weissman, A.M., Lewis, J., Chandrasekharappa, S.C., Chitnis, A.B., 2003. Mind Bomb is a ubiquitin ligase that is essential for efficient activation of Notch signaling by Delta. Dev. Cell 4, 67–82.
Jensen, J., 2004. Gene regulatory factors in pancreatic development. Dev. Dyn. 229, 176–200.
Jensen, J., Pedersen, E.E., Galante, P., Hald, J., Heller, R.S., Ishibashi, M., Kageyama, R., Guillemot, F., Serup, P., Madsen, O.D., 2000. Control of endodermal endocrine development by Hes-1. Nat. Genet. 24, 36–44.
Jonsson, J., Carlsson, L., Edlund, T., Edlund, H., 1994. Insulin-promoter-factor 1 is required for pancreas development in mice. Nature 371, 606–609.
Kawaguchi, Y., Cooper, B., Gannon, M., Ray, M., MacDonald, R.J., Wright, C.V.E., 2002. The role of the transcriptional regulator PTF1-p48 in converting intestinal to pancreatic progenitors. Nat. Genet. 32, 128–134.
Krapp, A., Knofler, M., Ledermann, B., Burki, K., Berney, C., Zoerkler, N., Hagenbuchle, O., Wellauer, P.K., 1998. The bHLH protein PTF1-p48 is essential for the formation of the exocrine and the correct spatial organization of the endocrine pancreas. Genes Dev. 12, 3752–3763.
Kumar, M., Melton, D., 2003. Pancreas specification: a budding question. Curr. Opin. Genet. Dev. 13, 401–407.
Kumar, M., Jordan, N., Melton, D., Grapin-Botton, A., 2003. Signals from lateral plate mesoderm instruct endoderm toward a pancreatic fate. Dev. Biol. 259, 109–122.
Lewis, M.J., Lewis III, E.H., Amos, J.A., Tsongalis, G.J., 2003. Cystic fibrosis. Am. J. Clin. Pathol. 120, S3–S13 (Suppl.).
Li, Z., Manna, P., Kobayashi, H., Spilde, T., Bhatia, A., Preuett, B., Prasadan, K., Hembree, M., Gittes, G.K., 2004. Multifaceted pancreatic mesenchymal control of epithelial lineage selection. Dev. Biol. 269, 252–263.
Lin, J.W., Biankin, A.V., Horb, M.E., Ghosh, B., Prasad, N.B., Yee, N.S., Pack, M.A., Leach, S.D., 2004. Differential requirement for ptf1a in endocrine and exocrine lineages of developing zebrafish pancreas. Dev. Biol. 270, 474–486.
Lorent, K., Yeo, S.Y., Oda, T., Chandrasekharappa, S., Chitnis, A., Matthews, R.P., Pack, M., 2004. Inhibition of Jagged-mediated Notch signaling disrupts zebrafish biliary development and generates multi-organ defects compatible with an Alagille syndrome phenocopy. Development 131, 5753–5766.
Mayer, A.N., Fishman, M.C., 2003. *nil per os* encodes a conserved RNA recognition motif protein required for morphogenesis and cytodifferentiation of digestive organs in zebrafish. Development 130, 3917–3928.
Miralles, F., Czernichow, P., Ozaki, K., Itoh, N., Scharfmann, R., 1999. Signaling through fibroblast growth factor receptor 2b plays a key role in the development of the exocrine pancreas. Proc. Natl. Acad. Sci. U. S. A. 96, 6267–6272.
Miyamoto, Y., Maitra, A., Ghosh, B., Zechner, U., Argani, P., Iacobuzio-Donahue, C.A., Sriuranpong, V., Iso, T., Meszoely, I.M., Wolfe, M.S., Hruban, R.H., Ball, D.W., Schmid, R.M., Leach, S.D., 2003. Notch mediates TGF alpha-induced changes in epithelial differentiation during pancreatic tumorigenesis. Cancer Cell 3, 565–576.
Murtaugh, L.C., Stanger, B.Z., Kwan, K.M., Melton, D.A., 2003. Notch signaling controls multiple steps of pancreatic differentiation. Proc. Natl. Acad. Sci. U. S. A. 100, 14920–14925.
Norgaard, G.A., Jensen, J.N., Jensen, J., 2003. FGF10 signaling maintains the pancreatic progenitor cell state revealing a novel role of Notch in organ development. Dev. Biol. 264, 323–338.
Obata, J., Yano, M., Mimura, H., Goto, T., Nakayama, R., Mibu, Y., Oka, C., Kawaichi, M., 2001. p48 subunit of mouse PTF1 binds to RBP-JK/CBF-1, the intracellulcar mediator of Notch signaling, and is expressed in the neural tube of early stage embryos. Genes Cells 6, 345–360.
Offield, M.F., Jetton, T.L., Labosky, P.A., Ray, M., Stein, R.W., Magnuson, M.A., Hogan, B.L.M., Wright, C.V.E., 1996. PDX-1 is required for pancreatic outgrowth and differentiation of the rostral duodenum. Development 122, 983–995.
Pack, M., Solnica-Krezel, L., Malicki, J., Neuhauss, S.C.F., Schier, A.F., Stemple, D.L., Driever, W., Fishman, M., 1996. Mutations affecting development of zebrafish digestive organs. Development 123, 321–328.
Piccoli, D.A., Spinner, N.B., 2001. Alagille syndrome and the Jagged1 gene. Semin. Liver Dis. 21, 525–534.
Pictet, R., Rutter, W.J., 1972. Development of embryonic endocrine pancreas. In: Steiner, D.F., Freinkel, N. (Eds.), Handbook of Physiology, Section 7: Endocrinology, vol. 1. American Physiological Society, Washington, DC, pp. 25–66.
Pictet, R.L., Clark, W.R., Williams, R.H., Rutter, W.J., 1972. An ultrastructural analysis of the developing embryonic pancreas. Dev. Biol. 29, 436–467.
Pin, C.L., Rukstalis, J.M., Johnson, C., Konieczny, S.F., 2001. The bHLH transcription factor Mist1 is required to maintain exocrine pancreas cell organization and acinar cell identity. J. Cell Biol. 155, 519–530.
Scarpelli, D.G., Rao, M.S., Reddy, J.K., 1991. Are acinar cells involved in

the pathogenesis of ductal adenocarcinoma of the pancreas? Cancer Cells 3, 275–277.
Scheer, N., Groth, A., Hans, S., Campos-Ortega, J.A., 2001. An instructive function for Notch in promoting gliogenesis in the zebrafish retina. Development 128, 1099–1107.
Schier, A.F., Neuhauss, S.C.F., Harvey, M., Malicki, J., Solnica-Krezel, L., Stainier, D.Y.R., Zwartkruis, F., Abdelilah, S., Stemple, D.L., Rangini, Z., Yang, H., Driever, W., 1996. Mutations affecting the development of the embryonic zebrafish brain. Development 123, 165–178.
Slack, J.M.W., 1995. Developmental biology of the pancreas. Development 121, 1569–1580.
Steer, M.L., 1997. Pathogenesis of acute pancreatitis. Digestion 58 (Suppl. 1), 46–49.
Wagner, D.S., Dosch, R., Mintzer, K.A., Wiemelt, A.P., Mullins, M.C., 2004. Maternal control of development at the midblastula transition and beyond: mutants from the zebrafish II. Dev. Cell 6, 781–790.
Wallace, K.N., Pack, M., 2003. Unique and conserved aspects of gut development in zebrafish. Dev. Biol. 255, 12–29.
Wallace, K.N., Shafinaz, A., Smith, E.M., Lorent, K., Pack, M., 2005. Intestinal growth and differentiation in zebrafish. Mech. Dev. 122, 157–173.
Warga, R.M., Nusslein-Volhard, C., 1999. Origin and development of the zebrafish endoderm. Development 126, 827–838.
Wendik, B., Maier, E., Meyer, D., 2004. Zebrafish mnx genes in endocrine and exocrine pancreas formation. Dev. Biol. 268, 372–383.
Wessells, N.K., Cohen, J.H., 1967. Early pancreas organogenesis: morphogenesis, tissue interactions, and mass effects. Dev. Biol. 15, 237–270.
Westerfield, M., 2000. The Zebrafish Book. Guide for the Laboratory Use of Zebrafish (*Danio rerio*), 4th ed. University of Oregon Press, Eugene, OR.
Yee, N.S., Pack, M., 2004. Zebrafish as a model for pancreatic cancer research. Methods Mol. Med. 103, 273–298.
Yee, N.S., Yusuff, S., Pack, M., 2001. Zebrafish pdx1 morphant displays defects in pancreas development and digestive organ chirality, and potentially identifies a multipotent pancreas progenitor cell. Genesis 30, 137–140.
Yee, N.S., Furth, E.E., Pack, M., 2003. Clinicopathologic and molecular features of pancreatic adenocarcinoma associated with Peutz–Jeghers Syndrome. Cancer Biol. Ther. 2, 38–47.
Youson, J.H., Al-Mahrouki, A.A., 1999. Ontogenetic and phylogenetic development of the endocrine pancreas (islet organ) in fishes. Gen. Comp. Endocrinol. 116, 303–335.
Zecchin, E., Mavropoulos, A., Devos, N., Filippi, A., Tiso, N., Meyer, D., Peers, B., Bortolussi, M., Argenton, F., 2004. Evolutionary conserved role of *ptf1a* in the specification of exocrine pancreatic fates. Dev. Biol. 268, 174–184.